

1 ~~The non-monotonicity of moist adiabatic warming~~ Non-monotonicity of
2 Moist-Adiabatic Warming

3 Osamu Miyawaki^a

4 ^a*Department of Geosciences, Union College, Schenectady New York, USA*

5 Corresponding author: Osamu Miyawaki, miyawako@union.edu

6 ABSTRACT: The moist adiabat is a foundational model of moist thermodynamics that is used
7 to understand convection, climate sensitivity, and the tropical temperature response to warming.
8 While surface saturation specific humidity increases monotonically with temperature following the
9 Clausius-Clapeyron relation, moist-adiabatic warming varies non-monotonically with initial sur-
10 face temperature. Here, we explain the physical mechanism of this non-monotonicity. It emerges
11 from a competition between two limiting factors on the condensation rate of rising air: the avail-
12 ability of water vapor and adiabatic cooling. At low temperatures, condensation is limited by water
13 vapor and warming increases with initial surface temperature. At high temperatures, condensation
14 is limited by adiabatic cooling, which is increasingly offset by the latent heat released from conden-
15 sation. In other words, the moist enthalpy response to warming transitions from being dominated
16 by an increase in sensible enthalpy (warming) to an increase in latent enthalpy (moistening). The
17 criterion where this transition occurs is $L_v \partial_T q^* = c_{pd}$, i.e. where the temperature sensitivity of
18 latent enthalpy equals that of sensible enthalpy. We show this non-monotonicity propagates to buoy-
19 ancy and updraft velocity using a zero-buoyancy plume model. The non-monotonicity in updraft
20 velocity predicted by the theory is qualitatively consistent with that simulated by cloud-resolving
21 models.

22 **1. Introduction**

23 The Clausius-Clapeyron relation ~~describes implies~~ the potential for a warmer atmosphere to
24 hold more water vapor (?). This principle is the basis for the positive water vapor feedback,
25 ~~first quantified in early climate models (?), and for an increase in the latent heat released during~~
26 ~~convection as the climate warms. Consistent with these principles, the total latent heat released from~~
27 ~~convection increases monotonically with surface temperature (Fig. ??a).~~ (?) It also underpins
28 ~~various scaling theories for climate responses to warming, including extreme precipitation, the~~
29 ~~Hadley cell edge, jet stream position, tropopause height, and convective available potential energy~~
30 ~~(CAPE; ???).~~

31 In the tropics, convection couples the surface ~~with to~~ the free troposphere. ~~Radiative cooling,~~
32 ~~which acts to destabilize the atmosphere to convection, acts on slower timescales (order of days)~~
33 ~~compared to convection (order of hours).~~ As a result, the tropical atmosphere is to first order
34 ~~in a state of quasi-equilibrium where the climatological free-tropospheric temperature follows a~~
35 ~~convectively neutral profile set by the surface temperature and humidity ?.~~ Although processes
36 like convective entrainment influence the details of this coupling (?), ~~moist adiabatic adjustment~~
37 ~~serves as (??), moist adiabatic adjustment is~~ a useful first-order approximation (?). The top-heavy
38 warming profile predicted by ~~moist adiabatic~~ ~~moist adiabatic~~ adjustment (Fig. ??b) is a robust
39 feature in climate models and observations, despite historical challenges in observational records
40 (??).

41 ~~This warming profile~~ The top-heavy warming profile predicted by the moist adiabat is important
42 because it increases ~~atmospheric static stability, which influences convection (?)~~ dry static stability.
43 Spatial variations in dry static stability influence the structure of tropical convergence zones
44 because horizontal free-tropospheric gradients, while weak, exist (??). This structure also defines
45 the tropical lapse rate feedback, a key negative feedback for global climate sensitivity (?). Given
46 ~~the monotonic increase in total latent heating~~ The lapse rate feedback partially cancels the water
47 vapor feedback and scales in tandem because amplified warming in the upper troposphere is a
48 consequence of increased surface water vapor and latent heat release (?). In a moist-adiabatic
49 atmosphere that is saturated at the surface, total latent heat release is $L_v(q_s^* - q_{top}^*)$ where L_v is
50 the latent heat of vaporization, q_s^* is surface saturation specific humidity, and q_{top}^* is the cloud top
51 saturation specific humidity. $q_{top}^* \rightarrow 0$ as $T \rightarrow 0$ in a moist-adiabatic atmosphere because the moist

adiabat does not predict a stratosphere¹. Thus we expect total latent heat release in a moist-adiabatic atmosphere to scale as q_s^* , which increases monotonically with surface temperature as expected from the Clausius-Clapeyron relation (Fig. ??a).

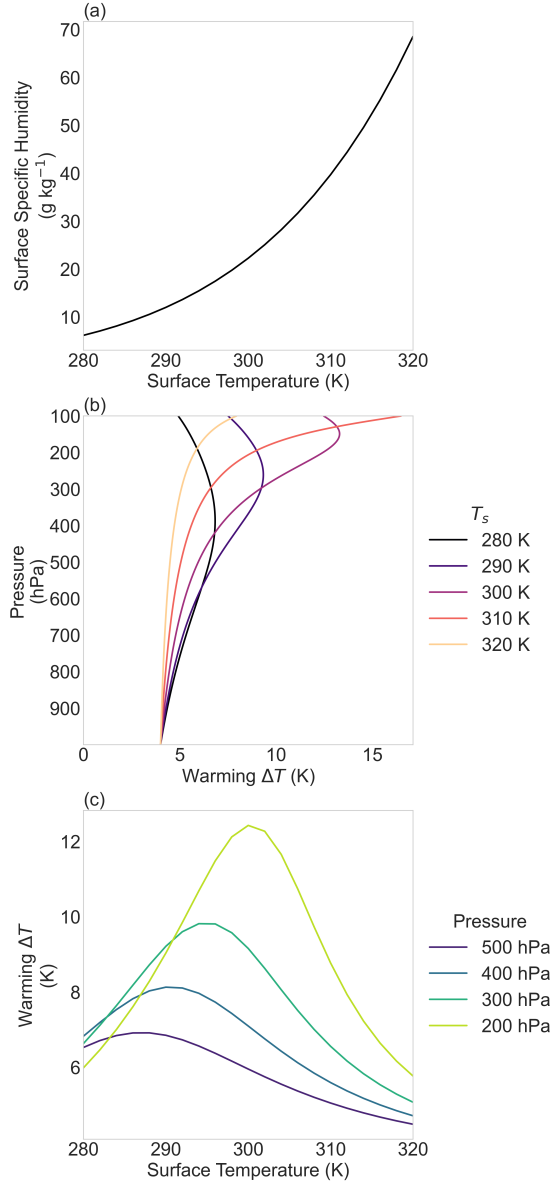
Given the monotonic increase in surface specific humidity with temperature, one might expect moist-adiabatic warming to also be monotonic with increase monotonically with the initial surface temperature at all heights levels. However, if moist-adiabatic warming is a non-monotonic function of surface temperature at a fixed height initial surface temperature (Fig. ??c). This (see Appendix A for details on calculating the moist adiabat). The non-monotonicity is independent of the vertical coordinate emerges in height coordinates (Fig. ??). While ? showed, with or without latent heat of fusion (see Appendix B and Fig. ??), and across different empirical formula for saturation vapor pressure (see Appendix C and Fig. ??). While previous work has acknowledged the existence of this non-monotonicity and its influence on zonal stationary circulations, a physical explanation for the non-monotonicity in moist adiabatic warming currently does not (??), an explanation does not yet exist in the literature.

This raises the question: What physical mechanism drives this non-monotonic warming? This paper presents a thermodynamic explanation for the origins of the non-monotonicity of moist-adiabatic warming? Here we explain the origin of the non-monotonicity in moist adiabatic moist-adiabatic warming and its cascading effects on other convective properties. Section 2 develops the theory of non-monotonic warming. Section 3 explores the implications of this non-monotonicity for the dynamics of moist convection. Section 4 provides a summary and discussion buoyancy and vertical velocity.

2. Theory of Non-Monotonic Warming

The non-monotonic relationship between upper-tropospheric warming and surface temperature (Fig. ??) can be explained by analyzing the sensitivity of the moist adiabatic lapse rate, Γ_m , to changes in surface temperature, T_s . To illustrate this, we start by defining the temperature profile, $T(z)$, in terms of its surface value, $T(0)$, and the lapse rate, $\Gamma(z) = -dT/dz$: moist-adiabatic temperature profile in pressure coordinates $T(p)$ in terms of the moist-adiabatic lapse rate

¹A more accurate proxy would consider how q_{top}^* varies with T_s . Assuming a fixed tropopause temperature = 200 K, q_{top}^* scales faster than Clausius-Clapeyron because of decreasing cloud top pressure with warming (?).



73 FIG. 1. (a) The change in column-integrated Surface saturation specific humidity (Δq_s) resulting from a
74 4 K increases monotonically with surface warming as a function of surface temperature (T_s). (b) Vertical
75 profiles of the moist adiabatic temperature response (ΔT) moist-adiabatic warming to a 4 K surface warming
76 for $T_s = 280, 290, 300, 310$, and 320 K. Warming decreases with initial surface temperature at lower levels
77 while it increases with initial surface temperature at higher levels. (c) The moist-adiabatic warming (ΔT) varies
78 non-monotonically with initial surface temperature at 5 all levels, 10 e.g. at 500, 15 400, and 20 km as a function of
79 T_s 300, showing a non-monotonic response where and 200 hPa. moist-adiabatic warming peaks at an intermediate
80 temperature warmer initial surface temperatures at higher levels.

87 $\Gamma_m \equiv dT/dp$:

$$T(z, p) = T(0, p_s) + \int_{0, p_s}^{z, p} \Gamma(z, p') dz' \quad (1)$$

88 We apply Eq. (??) to a base state with surface temperature where T_s and a perturbed state with
 89 surface temperature $T_s + \Delta T_s$. The warming at any height, $\Delta T(z)$, is the difference between these
 90 two profiles, $\Delta T(z) = T_{\text{pert}}(z) - T_{\text{base}}(z)$, which yields: is surface temperature. We assume the
 91 atmosphere is saturated from the surface. The difference between a perturbed and baseline state
 92 (Δ) then follows as

$$\Delta T(z, p) = \Delta T_s \pm \int_{0, p_s}^{z, p} \Delta \Gamma(z, p') dz' \quad (2)$$

93 where $\Delta \Gamma = \Gamma_{\text{pert}} - \Gamma_{\text{base}}$. For a small perturbation, the change in the lapse rate, $\Delta \Gamma$, $\Delta \Gamma_m$ can be
 94 approximated using a first-order Taylor expansion: $\Delta \Gamma \approx \frac{d\Gamma_m}{dT_s} \Delta T_s \Delta \Gamma_m \approx \frac{d\Gamma_m}{dT_s} \Delta T_s$. Substituting this
 95 into Eq. (??) gives: ??) gives

$$\Delta T(z, p) \approx \Delta T_s \pm \left(\int_{0, p_s}^{z, p} \frac{d\Gamma_m}{dT_s} dz dp' \right) \Delta T_s \quad (3)$$

96 This establishes that the vertical structure of the warming anomaly (i.e., its deviation from the
 97 uniform surface warming) The non-monotonicity in moist-adiabatic warming is encoded into
 98 $d\Gamma_m/dT_s$, the sensitivity of the moist-adiabatic lapse rate to surface temperature. Indeed, $d\Gamma_m/dT_s$
 99 is controlled by the vertical integral of non-monotonic with respect to temperature, with a local
 100 minimum that varies as a function of surface temperature and pressure (dashed line in Fig. ??a).
 101 $d\Gamma_m/dT_s$ is mostly negative in the troposphere (Fig. ??b). This is consistent with amplified
 102 warming aloft because the integral in Eq. (??) is from high to low pressure, which introduces a
 103 negative sign.

104 Γ_m is a function of local temperature and pressure $\Gamma_m(T, p)$. To understand $d\Gamma_m/dT_s$, the
 105 sensitivity of the lapse rate to the we rewrite it in terms of local state variables (T, p) using the
 106 chain rule:

$$\frac{d\Gamma_m}{dT_s} = \left(\frac{\partial \Gamma_m}{\partial T} \right)_p \cdot \frac{dT}{dT_s} + \left(\frac{\partial \Gamma_m}{\partial p} \right)_T \cdot \frac{dp}{dT_s} \quad (4)$$

107 The second term $\frac{dp}{dT_s} = 0$ because pressure, being the vertical coordinate, is independent of surface
 108 temperature. Therefore, understanding the physical mechanisms that determine this sensitivity is

¹⁰⁹ the key to explaining the By definition $\Gamma_m = \frac{dT}{dp}$, so

$$\frac{d}{dp} \left(\frac{dT}{dT_s} \right) = \left(\frac{\partial \Gamma_m}{\partial T} \right)_p \cdot \frac{dT}{dT_s} \quad (5)$$

¹¹⁰ This is an ordinary differential equation for $\frac{dT}{dT_s}$ as a function of pressure. The solution with the
¹¹¹ boundary condition $\frac{dT}{dT_s}(p_s) = 1$, is

$$\frac{dT}{dT_s} = \exp \left(\int_{p_s}^p \left(\frac{\partial \Gamma_m}{\partial T} \right)_p dp' \right) \quad (6)$$

¹¹² Substituting Eq. (??) into Eq. (??) gives

$$\frac{d\Gamma_m}{dT_s} = \left(\frac{\partial \Gamma_m}{\partial T} \right)_p \cdot \exp \left(\int_{p_s}^p \left(\frac{\partial \Gamma_m}{\partial T} \right)_{p'} dp' \right) \quad (7)$$

¹¹³ where $(\partial \Gamma_m / \partial T)_p$ is the moist-adiabatic lapse rate sensitivity to local temperature T at pressure
¹¹⁴ level p . The integral describes how a small surface temperature perturbation dT_s influences
¹¹⁵ $\Gamma_m(T, p)$ through the sum of all Γ_m changes that occur below pressure level p .

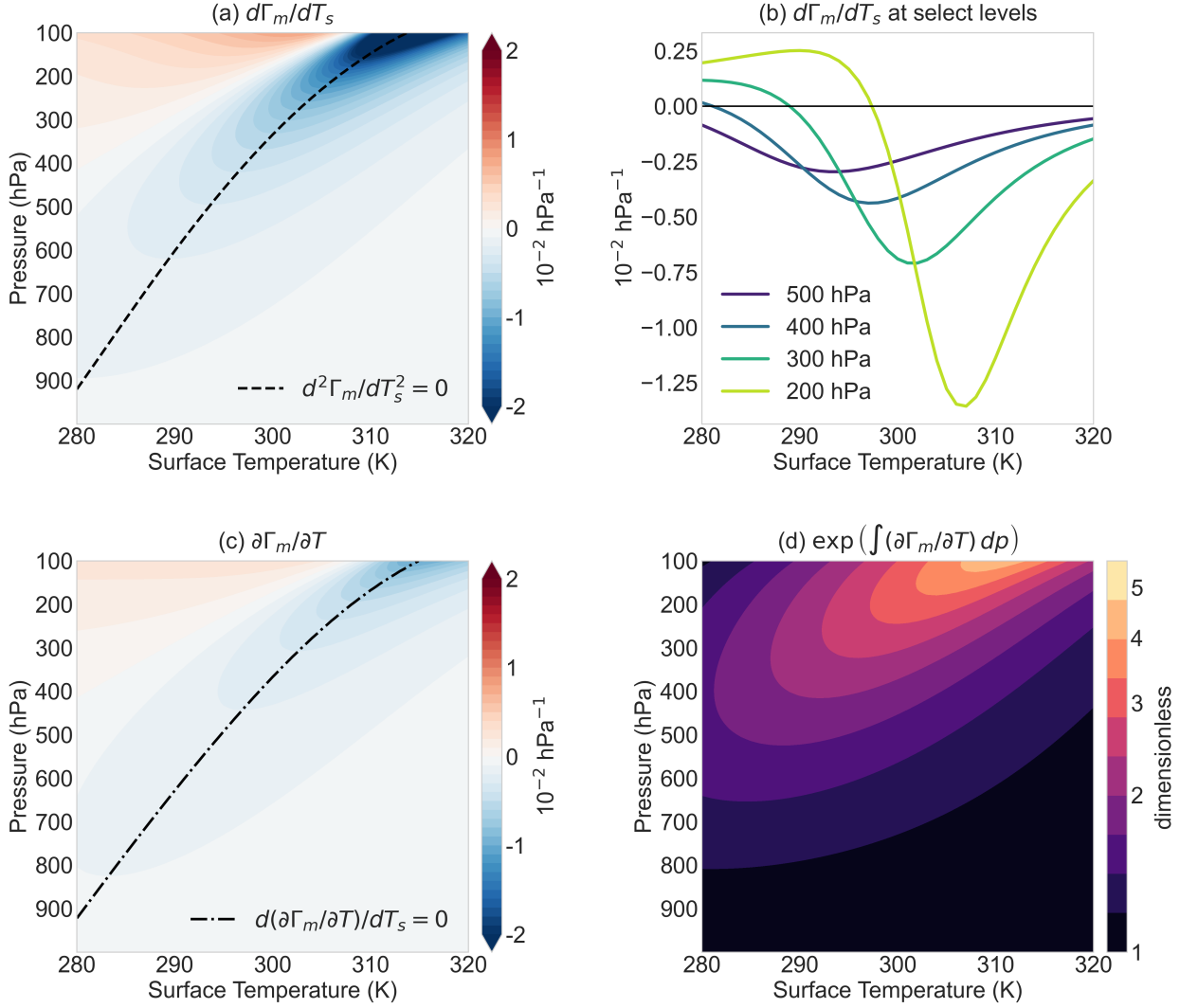
¹¹⁶ The non-monotonicity of moist-adiabatic warming can emerge from

- ¹¹⁷ 1. $\partial \Gamma_m / \partial T$ being non-monotonic and the integral acting to amplify it, or
- ¹¹⁸ 2. $\partial \Gamma_m / \partial T$ being monotonic but sign changes in $\partial \Gamma_m / \partial T$ leads to the integral being
¹¹⁹ non-monotonic.

¹²⁰ Numerical solutions show that $\partial \Gamma_m / \partial T$ is non-monotonic, with a local minimum that varies as a
¹²¹ function of surface temperature and pressure (dash-dot line, $\partial \Gamma_m / \partial T$ in Fig. ??c). The integral
¹²² term amplifies this non-monotonicity (Fig. ??d).

¹²³ We begin by deriving an expression for the moist adiabatic lapse rate-

¹²⁴ Why is $\partial \Gamma_m / \partial T$ non-monotonic? To understand this we solve for Γ_m from the first law of
¹²⁵ thermodynamics for a-saturated, ascending air parcel, which is equivalent to the conservation of
¹²⁶ Moist Static Energy (MSE): adiabatic, non-precipitating, and reversible ascent of a saturated air



123 FIG. 2. (a) The sensitivity of the moist-adiabatic lapse rate to surface temperature, $d\Gamma_m/dT_s$, varies
 124 non-monotonically with surface temperature. (b) The local minimum of $d\Gamma_m/dT_s$ shifts toward warmer
 125 temperatures with surface temperature at higher levels. (c) The sensitivity of the moist-adiabatic lapse rate
 126 to the local temperature at pressure p , $\partial\Gamma_m/\partial T$, also varies non-monotonically with surface temperature. (d)
 127 The integral term in Eq. (??) amplifies the non-monotonicity of $\partial\Gamma_m/\partial T$. The surface temperature sensitivity of
 128 Γ_m (a) is the product of the local temperature sensitivity (c) and its integral (d), see Eq. (??).

133 parcel:

$$c_{\underline{p}} dT - \alpha dp + g dz + L_v dq_{\underline{s}}^* = 0 \quad (8)$$

134 Here, c_p where c_p is the specific heat capacity of dry air, g is the acceleration due to gravity, z
 135 is height, air at constant pressure, α is specific volume, L_v is the latent heat of vaporization, and
 136 $q_s q^*$ is the saturation specific humidity. To find the moist adiabatic lapse rate, $\Gamma_m = -dT/dz$, we
 137 divide. We assume

- 138 1. $c_p \approx c_{pd}$, neglecting the role of water of all phases on the specific heat capacity, and
 139 2. $\alpha \approx \alpha_d = R_d T/p$, neglecting the virtual effect of water vapor on density.

140 Next we use the chain rule to expand dq^* :

$$dq^* = \left(\frac{\partial q^*}{\partial T} \right)_p dT + \left(\frac{\partial q^*}{\partial p} \right)_T dp \quad (9)$$

141 Substituting Eq. (??) by dz :

$$c_p \frac{dT}{dz} + g + L_v \frac{dq_s}{dz} = 0$$

142 ?? into Eq. ?? and rearranging gives

$$\left(c_{pd} + L_v \left(\frac{\partial q^*}{\partial T} \right)_p \right) dT = \left(\alpha_d - L_v \left(\frac{\partial q^*}{\partial p} \right)_T \right) dp \quad (10)$$

143 Substituting $dT/dz = -\Gamma_m$ and solving for Γ_m yields:

$$\Gamma_m = \frac{g}{c_p} + \frac{L_v}{c_p} \frac{dq_s}{dz} = \Gamma_d + \frac{L_v}{c_p} \frac{dq_s}{dz}$$

144 We can derive closed-form expressions for the q^* derivatives using the Clausius-Clapeyron relation
 145 and Dalton's Law. These q^* derivatives describe the role of phase equilibrium shifts in q^* with T
 146 and p on the effective heat capacity and specific volume of the air parcel, respectively:

$$c_L \equiv L_v \left(\frac{\partial q^*}{\partial T} \right)_p \approx \frac{L_v^2 q^*}{R_v T^2} \quad (11)$$

$$\alpha_L \equiv -L_v \left(\frac{\partial q^*}{\partial p} \right)_T \approx \frac{L_v q^*}{p} \quad (12)$$

147 where Γ_d is the dry adiabatic lapse rate. For simplicity, and following common theoretical
 148 practice, Γ_d , L_v , and c_p are assumed to be constant. Then the sensitivity of the lapse rate to surface
 149 temperature is controlled entirely by the sensitivity of the vertical moisture gradient:

$$\frac{d\Gamma_m}{dT_s} = \frac{L_v}{c_p} \frac{d}{dT_s} \left(\frac{dq_s}{dz} \right)$$

150 We can decompose the moisture gradient, dq_s/dz , into two components using the chain rule, as q_s
 151 is a function of temperature T and pressure p approximation comes from assuming that saturation
 152 vapor pressure $e^* \ll p$.

153 We interpret c_L as a latent heat capacity, which represents the increase in thermal inertia as latent
 154 heating cancels part of the cooling from expansion. c_L acts to increase the heat capacity of the air
 155 parcel such that it has an effective heat capacity $c_{pd} + c_L$.

156 We interpret α_L as a latent specific volume, which represents the enhanced expansion of air with
 157 ascent as lower pressure shifts the phase equilibrium of water toward the vapor phase. α_L acts to
 158 increase the volume of air such that it has an effective specific volume $\alpha_d + \alpha_L$.

159 Solving for the moist-adiabatic lapse rate $\Gamma_m = dT/dp$:

$$\frac{dq_s}{dz} = \frac{\partial q_s}{\partial T} \frac{dT}{dz} + \frac{\partial q_s}{\partial p} \frac{dp}{dz}$$

160

$$\Gamma_m = \frac{dT}{dp} = \frac{\alpha_d + \alpha_L}{c_{pd} + c_L} \quad (13)$$

$$= \Gamma_d \cdot \frac{1 + \frac{\alpha_L}{\alpha_d}}{1 + \frac{c_L}{c_{pd}}} \quad (14)$$

161 Substituting the definitions of the moist lapse rate ($dT/dz = -\Gamma_m$) and hydrostatic balance
 162 ($dp/dz = -\rho g$, where ρ is $\Gamma_d = \alpha_d/c_{pd}$ is the density of air) allows the moisture gradient to be
 163 expressed as the sum of a Cooling Term and a Pressure Term: dry adiabatic lapse rate in pressure
 164 coordinates and the two non-dimensional terms represent the fractional increase in effective specific
 165 heat capacity and specific volume due to the pressure and temperature sensitivities of the phase

$$\tilde{c} = \frac{c_L}{c_{pd}} = \frac{L_v^2 q^*}{c_{pd} R_v T^2} \quad (15)$$

$$\tilde{\alpha} = \frac{\alpha_L}{\alpha_d} = \frac{L_v q^*}{R_d T} = \frac{R_v c_{pd} T}{R_d L_v} \tilde{c} = k \tilde{c} \quad (16)$$

167 Substituting Eq. (??) and Eq. (??) into Eq. (??) gives

$$\Gamma_m = \Gamma_d \cdot \frac{1 + k \tilde{c}}{1 + \tilde{c}} \quad (17)$$

168 For typical values in Earth's atmosphere ($R_v = 461 \text{ J kg}^{-1} \text{ K}^{-1}$, $R_d = 287 \text{ J kg}^{-1} \text{ K}^{-1}$,
169 $c_{pd} = 1005 \text{ J kg}^{-1} \text{ K}^{-1}$, $L_v = 2.5 \times 10^6 \text{ J kg}^{-1}$, and $T \in [200, 320] \text{ K}$), the factor
170 $k = \frac{R_v c_{pd} T}{R_d L_v} \in [0.13, 0.21]$. k is a weak function of temperature and is a quasi-constant of order 10^{-1} .
171 In contrast, \tilde{c} scales exponentially with temperature (through q^*) and varies from $\tilde{c}(200 \text{ K}) \sim 10^{-4}$
172 to $\tilde{c}(320 \text{ K}) \sim 10^1$. The temperature sensitivity of Γ_m is controlled by \tilde{c} . In the dry limit $\tilde{c} \rightarrow 0$,
173 $\Gamma_m \rightarrow \Gamma_d$. In the moist limit $\tilde{c} \rightarrow \infty$, $\Gamma_m \rightarrow k \Gamma_d \sim 0.1 \Gamma_d$, so the moist adiabat cools slowly with
174 height². Because Γ_m is bounded, the magnitude of $\partial \Gamma_m / \partial T$ must peak at some intermediate \tilde{c} .

175 Where does the magnitude of $\partial \Gamma_m / \partial T$ reach its peak value? To solve this we use the quotient
176 rule on Eq. (??):

$$\frac{dq_s}{dz} \frac{\partial \Gamma_m}{\partial T} = \underbrace{\frac{1}{c_{pd} + c_L} \frac{\partial(\alpha_d + \alpha_L)}{\partial T}}_{\text{Cooling Term}} \underbrace{\frac{1}{c_{pd} + c_L} \frac{\partial}{\partial T} \left(\frac{\alpha_d + \alpha_L}{(c_{pd} + c_L)^2} \frac{\partial c_L}{\partial T} \right)}_{\text{latent volume sensitivity}} + \underbrace{\frac{1}{c_{pd} + c_L} \frac{\partial}{\partial T} \left(-\frac{\alpha_d + \alpha_L}{(c_{pd} + c_L)^2} \frac{\partial c_L}{\partial T} \right)}_{\text{Pressure Term}} \underbrace{\frac{1}{c_{pd} + c_L} \frac{\partial}{\partial T} \left(\frac{\alpha_d + \alpha_L}{(c_{pd} + c_L)^2} \frac{\partial c_L}{\partial T} \right)}_{\text{latent heat capacity}} \quad (18)$$

177 The Cooling Term represents the decrease in water vapor latent volume sensitivity varies
178 monotonically with surface temperature (Fig. ??a, c). The non-monotonicity is due to the parcel
179 cooling as it rises and expands. The Pressure Term represents the increase in water vapor due to
180 the decrease in ambient pressure as the parcel rises. Substituting this decomposition back into

²This breaks down because the assumption $e^* \ll p$ is poor in a steam atmosphere where water vapor becomes a significant fraction of the atmosphere's mass, i.e. saturation mixing ratio $r^* \gtrsim 1$. At surface pressure this corresponds to $T \gtrsim 360 \text{ K}$.

181 latent heat capacity sensitivity (Fig. ??b, d) so we further decompose it to identify its origin:

$$-\frac{\alpha_d + \alpha_L}{(c_{pd} + c_L)^2} \frac{\partial c_L}{\partial T} = -\frac{1}{p} \cdot (1 + \tilde{\alpha}) \cdot \frac{R_d}{c_{pd}} \frac{\partial \log c_L}{\partial \log T} \cdot f_d \cdot f_L \quad (19)$$

182 where

$$f_d \equiv c_d / (c_{pd} + c_L) \quad (20)$$

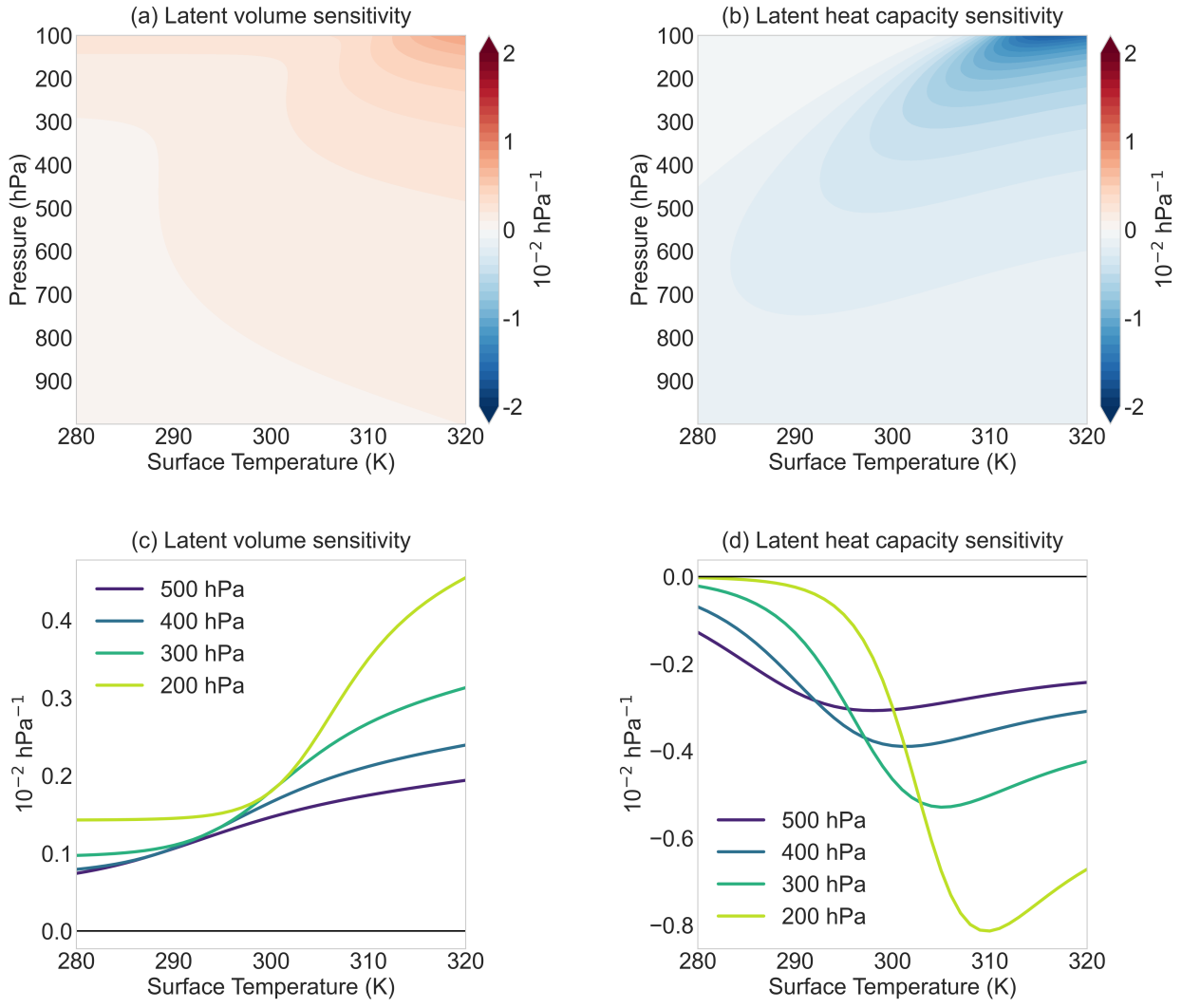
$$f_L \equiv c_L / (c_{pd} + c_L) \quad (21)$$

184 and $f_d + f_L = 1$. f_d and f_L represent the sensible and latent fractions of effective heat capacity,
185 respectively. f_d quantifies the fraction of the moist enthalpy change associated with an increase
186 in sensible enthalpy (i.e. warming) while f_L quantifies the fraction associated with an increase in
187 latent enthalpy (i.e. moistening).

194 Eq. (??) allows us to decompose the total sensitivity, $d\Gamma_m/dT_s$, into the sum of contributions
195 from these two terms. They have opposing effects on the total sensitivity (??) shows the latent heat
196 capacity sensitivity is a product of four terms that vary monotonically with T . $\tilde{\alpha} = L_v q^*/(\alpha_d p)$
197 scales exponentially with T through q^* (dashed line in Fig. ??a). The Cooling Term acts to
198 decrease Γ_m with warming (fractional change in latent heat capacity to a fractional change in
199 temperature $\partial \log c_L / \partial \log T = L_v / (R_v T) - 2$ decreases with T (dotted line in Fig. ??b), while the
200 Pressure Term acts to increase Γ_m with warming (??a). The product of these two terms is weakly
201 non-monotonic in T with a local minimum located approximately where $\tilde{\alpha} = R_v T / L_v$ (white line
202 in Fig. ??e).

203 The opposing effects of ??b). At low T , $\tilde{\alpha}$ is small so the product is dominated by the decrease in
204 $\partial \log c_L / \partial \log T$. At high T , $\tilde{\alpha}$ is large so the product is dominated by the exponential increase in $\tilde{\alpha}$
205 . However, the non-monotonicity that emerges from these two terms on the lapse rate translate into
206 competing contributions to the overall warming profile. Integrating the Cooling Term's sensitivity
207 reveals a warming contribution that amplifies monotonically with increasing T_s at all heights (is not
208 the source of the peak magnitude in $\partial \Gamma_m / \partial T$, which requires a local maximum, not a minimum).

209 The sensible fraction of effective heat capacity f_d logically decreases with T because c_{pd} is
210 a constant while latent heat capacity c_L increases exponentially with T through q^* (red line in
211 Fig. ??a, ??b). In contrast, integrating the Pressure Term's sensitivity reveals a contribution that



188 FIG. 3. The moist-adiabatic lapse rate sensitivity to local temperature T , $\partial\Gamma_m/\partial T$ (Fig. ??c), is decomposed
 189 into contributions from (a) the latent volume sensitivity and (b) the latent heat capacity sensitivity following
 190 Eq. (??). (c) The latent volume sensitivity monotonically increases with local temperature T across
 191 all pressure levels, e.g. across 500, 400, 300, and 200 hPa. (d) The latent heat capacity sensitivity has a local
 192 minimum that shifts toward warmer surface temperature at higher levels, consistent with the behavior of $d\Gamma_m/dT_s$
 193 (Fig. ??b).

212 acts to cool the atmosphere relative to the surface, and this cooling effect becomes stronger as T_s
 213 increases (??c). The latent fraction of effective heat capacity f_L logistically increases with T (blue
 214 line in Fig. ??c). The product $f_d \cdot f_L$ peaks when $f_d = f_L$, or $c_L = c_{pd}$ (black line in Fig. ??d).

215 What is the physical intuition behind the peak occurring at $c_L = c_{pd}$? Recall that c_L quantifies the
 216 enhancement of effective heat capacity due to condensation heating offsetting adiabatic cooling.
 217 Condensation ($\partial_T q^*$ in c_L) requires two ingredients: 1) cooling from expansion and 2) water
 218 vapor. f_d and f_L correspond to the fractional availability of the two ingredients. At low T
 219 ($c_L < c_{pd}$), condensation is limited by the availability of water vapor (blue line in Fig. ??e, ??d).
 220 Physically, this occurs because a decrease in ambient pressure favors the vapor phase over condensed
 221 phases ??c). The moist enthalpy response to warming is dominated by an increase in sensible
 222 enthalpy (warming). At high T ($c_L > c_{pd}$), condensation is limited by adiabatic cooling (red line
 223 in Fig. ??c), which means the Pressure Term contributes to a decrease in latent heat release from
 224 condensation compared to a hypothetical alternative where temperature were to decrease without
 225 a corresponding decrease in pressure. The total warming anomaly, $\Delta T_{\text{anomaly}}(z) = \Delta T(z) - \Delta T_s$, is
 226 the sum of these two opposing effects:

$$\underline{\Delta T_{\text{cool}}(z) \approx -\Delta T_s \int_0^z \frac{d}{dT_s} \left(\frac{L_v}{c_p} \left(-\Gamma_m \frac{\partial q_s}{\partial T} \right) \right) dz'}$$

$$\underline{\Delta T_{\text{pres}}(z) \approx -\Delta T_s \int_0^z \frac{d}{dT_s} \left(\frac{L_v}{c_p} \left(-\rho g \frac{\partial q_s}{\partial p} \right) \right) dz'}$$

$$\underline{\Delta T_{\text{anomaly}}(z) = \Delta T_{\text{cool}}(z) + \Delta T_{\text{pres}}(z)}$$

227 The non-monotonic behavior of moist adiabatic warming is thus a consequence of the competition
 228 between these two opposing effects. rising parcel retains more water as vapor instead of
 229 condensation. The moist enthalpy response to warming is dominated by an increase in latent
 230 enthalpy (moistening). The peak in latent heat capacity sensitivity corresponds to where the
 231 availability of water vapor and cooling are equally limiting (black line in Fig. ??c). The
 232 non-monotonicity in $\partial \Gamma_m / \partial T$ and moist-adiabatic warming emerges from the competition between
 233 the two limiting factors of condensation, which controls the partitioning of the moist enthalpy
 234 response to warming into sensible and latent enthalpy.

235 The reason for the eventual dominance of the Pressure Term's temperature sensitivity lies in its
 236 temperature scaling relative to the Cooling Term. We can approximate the partial derivatives of

237 specific humidity using the Clausius-Clapeyron relation and the ideal gas law:

$$\frac{\partial q_s}{\partial T} \approx q_s \frac{L_v}{R_v T^2}$$

$$\frac{\partial q_s}{\partial p} \approx -\frac{q_s}{p}$$

238 where R_v is the gas constant for water vapor. Substituting these approximations into Eq. (??) gives:

$$\frac{dq_s}{dz} \approx -\Gamma_m \left(q_s \frac{L_v}{R_v T^2} \right) - \rho g \left(-\frac{q_s}{p} \right) \approx -q_s \left(\Gamma_m \frac{L_v}{R_v T^2} \right) + q_s \left(\frac{\rho g}{p} \right)$$

248 Using the ideal gas law for moist air, $p \approx \rho R_d T_v$ (where T_v is

249 How well does the condition $c_L = c_{pd}$ capture the actual peak in $\partial \Gamma_m / \partial T$? The theory
250 overpredicts the T_s where the virtual temperature), the pressure-related term in Eq. (??) can
251 be rewritten:

$$\frac{dq_s}{dz} \approx -q_s \left(\frac{\Gamma_m L_v}{R_v T^2} \right) + q_s \left(\frac{g}{R_d T_v} \right)$$

252 Both terms scale with the saturation specific humidity, q_s , which increases exponentially
253 with temperature. However, they are also multiplied by prefactors with different temperature
254 dependencies.

255 The Cooling Term is modulated by a prefactor that scales as $1/T^2$. This dampens the exponential
256 increase in the Cooling Term with surface warming. Γ_m in magnitude of $\partial \Gamma_m / \partial T$ peaks (compare
257 solid and dash-dot lines in Fig. ??). This error is due to the weak non-monotonicity in the
258 numerator of the Cooling Term prefactor further modulates the exponential increase because Γ_m
259 decreases with warming. The Pressure Term is modulated by a prefactor that scales as $1/T_v$. Thus
260 the Pressure Term prefactor is a weaker function of temperature than the Cooling Term prefactor
261 (product $(1+\tilde{\alpha})R_d/c_{pd}\partial \log(c_L)/\partial \log(T)$ which decreases with height (Fig. ??b)). The error
262 maximizes at the surface where the theory predicts a peak T_s that is 1.6 K warmer than the true
263 peak T_s .

264 The difference in T_s predicted by the theory and the true peak of Γ_m/dT_s grows with height
265 because the integral term in Eq. (??) amplifies the error in $\partial \Gamma_m / \partial T$ at each level below. This error

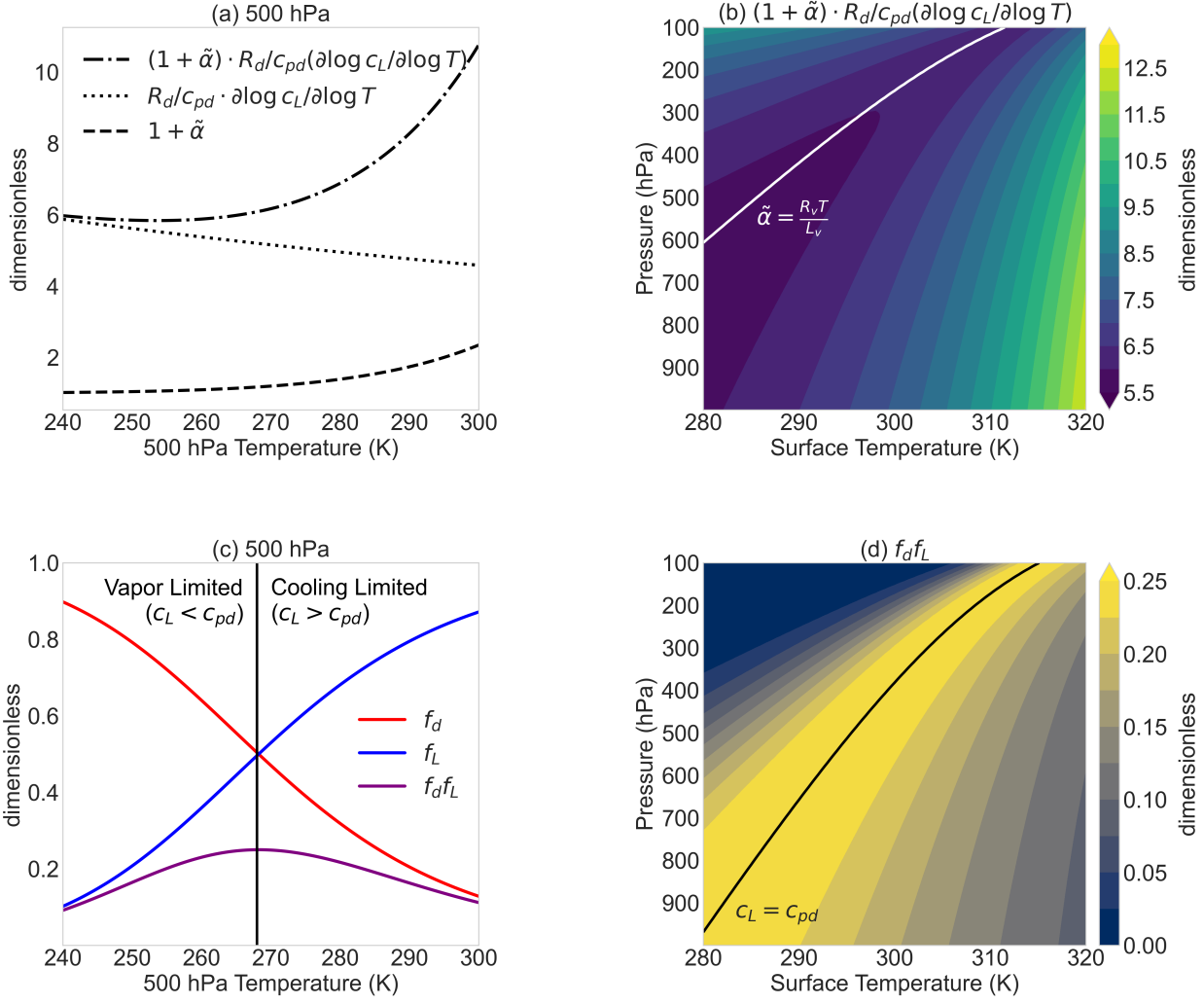


FIG. 4. The latent heat capacity sensitivity is decomposed into a product of four terms (Eq. ??) that vary monotonically with local temperature T , where local means at pressure p . (a) The latent volume ratio $\tilde{\alpha}$ increases exponentially with T (dashed) while the fractional change in latent heat capacity c_L to a fractional change in T decreases approximately linearly with T (dotted). The product of the two is weakly non-monotonic with T where the product has a local minimum (dash-dot). (b) The local minimum across the pressure-surface temperature space approximately occurs where $\tilde{\alpha} = R_v T / L_v$ (white line). (c) The latent fraction of effective heat capacity f_L increases logically with T (blue line) while the sensible fraction f_d decreases logically with T (red line). The product of the two is non-monotonic with T where the product has a local maximum (purple line). (d) The $f_d \cdot f_L$ local maximum across the pressure-surface temperature space occurs where $c_L = c_{pd}$ (black line).

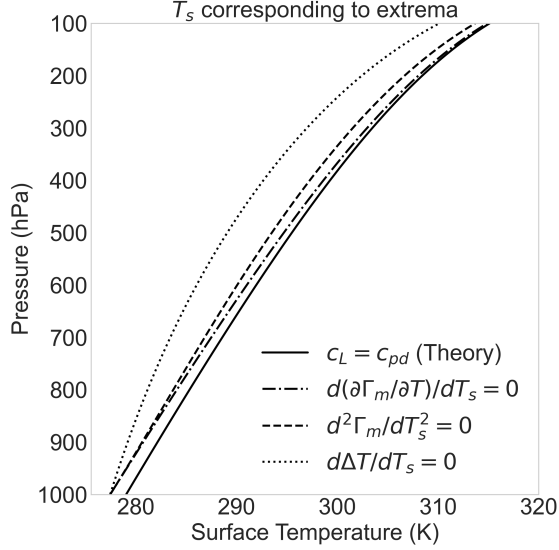
266 maximizes at 420 hPa where $c_L = c_{pd}$ predicts a peak T_s that is 2.0 K warmer than the true peak
267 T_s (compare solid and dashed lines in Fig. ??). Consequently, as ??). This error compounds for T_s
268 rises, the rapid decay of the Cooling Term's prefactor mutes the effect of increasing q_s relative to
269 the Pressure Term. This allows the Pressure Term's influence on the lapse rate to eventually catch up
270 to that of the Cooling Term. The differing sensitivities of these two terms to temperature cause the
271 warming to first strengthen and then weaken with of peak moist-adiabatic warming ΔT (Eq. ??),
272 leading to a maximum error of 6.6 K at 382 hPa (compare solid and dotted lines in Fig. ??). Thus
273 the condition $c_L = c_{pd}$ is a useful first-order estimate of the T_s where moist-adiabatic warming
274 peaks.

275 Warming is decomposed into contributions from the Cooling Term and the Pressure Term. (a)
276 The vertical profile of the warming contribution from the Cooling Term for select T_s . (b) The
277 warming contribution from the Cooling Term at fixed heights as a function of surface temperature.
278 This term provides a warming effect that increases monotonically with temperature. (c) The vertical
279 profile of the relative cooling contribution from the Pressure Term. (d) The relative cooling from
280 the Pressure Term at fixed heights. Both the Cooling and Pressure terms become stronger as the
281 surface temperature increases.

282 The (a) Cooling Prefactor, $\Gamma_m L_v / (R_v T^2)$, and (b) Pressure Prefactor, $g / (R_d T_v)$, as a function
283 of height and surface temperature. The Cooling Prefactor weakens strongly with temperature due
284 to its $1/T^2$ dependence. In contrast, the Pressure Prefactor weakens more slowly due to its $1/T_v$
285 dependence.

286 3. Implications of non-monotonicity in moist adiabatic warming on convection for Convective 287 Dynamics

288 The non-monotonic warming of a moist adiabat non-monotonicity of moist-adiabatic warming
289 has implications for the dynamics of convection convective dynamics. For example, ? showed that
290 parcel buoyancy at the tropopause is a non-monotonic function of surface temperature. Romps'
291 explanation is that as surface temperature increases the parcel's enthalpy anomaly is increasingly
292 partitioned into a latent enthalpy (moisture) anomaly rather than a sensible enthalpy (temperature)
293 anomaly. Since buoyancy is driven by the temperature anomaly between the rising parcel and
294 its environment, the shift from sensible to latent enthalpy anomaly with warming leads to the



275 FIG. 5. The sensitivity Surface temperature T_s corresponding to the criterion $c_L = c_{pd}$ (solid), the minimum of
 276 the moist adiabatic moist-adiabatic lapse rate sensitivity to a change in surface local temperature $\partial\Gamma_m/\partial T$ (dash
 277 dot), $\partial\Gamma_m/\partial T_s$, exhibits a non-monotonic structure as a function the minimum of height and the moist-adiabatic
 278 lapse rate sensitivity to surface temperature $d\Gamma_m/dT_s$ (adashed). This structure arises from the competition
 279 between two opposing physical effects. The Cooling Term (b), which represents and the effect maximum
 280 of condensation from adiabatic cooling, is a negative contribution at all temperatures. The Pressure Term
 281 moist-adiabatic warming ΔT (edotted), which represents. The theory most accurately captures the effect T_s
 282 corresponding to the minimum of decreasing pressure with height, is a positive contribution $\partial\Gamma_m/\partial T$. The
 283 non-monotonicity of discrepancy between the total sensitivity arises because theory and the positive contribution
 284 from the Pressure Term grows more rapidly with T_s than corresponding to the negative contribution from
 285 minimum of $d\Gamma_m/dT_s$ and ΔT is larger because the Cooling Term error at pressure p is the accumulation of errors
 286 at levels below p (see Eq. ?? and ??).

307 tropopause buoyancy and thus CAPE to peak at an intermediate temperature. Here, we provide an
 308 alternative perspective of the non-monotonicity in buoyancy based on the sensitivity of the vertical
 309 moisture gradient ($\frac{dq_s}{dz}$) to warming. Specifically the criterion where B peaks is $\beta = 2c_{pd}$ where

$$\beta = c_{pd} + L_v \frac{\partial q^*}{\partial T} = c_{pd} + c_L \quad (22)$$

310 Thus the ? criterion that maximizes B is equivalent to the criterion where moist-adiabatic warming
 311 peaks, $c_L = c_{pd}$. We show this is true if the entrainment parameter a is small and derive a more
 312 general criterion that maximizes buoyancy.

313 We model buoyancy (Buoyancy B) as is the normalized virtual temperature difference between
 314 a non-entraining parcel (or equivalently, density) difference between the rising parcel $T_{v,p}$ and
 315 the environment ($T_{v,e}$). For simplicity, we will. Here we neglect the virtual effects of water and
 316 use standard temperature:

$$B(z) \approx \frac{g}{T_e(z)} \frac{g}{T_e} (T_p(z) - T_e(z)) \quad (23)$$

317 As before, we express temperature profiles in terms of T_s and the integral of their respective lapse
 318 rates. We assume the parcel follows a moist adiabatic moist-adiabatic lapse rate, Γ_m , while the
 319 environment follows is neutrally buoyant with respect to an entraining lapse rate, Γ_e , following
 320 the zero-buoyancy plume model (?):

$$T_p(z) = T_s \pm \int_0^z \frac{dp}{p_s} \Gamma_m(z') dz dp' \quad (24)$$

$$T_e(z) = T_s \pm \int_0^z \frac{dp}{p_s} \Gamma_e(z') dz dp' \quad (25)$$

321 Substituting Eq. (??) and (??) into the definition of buoyancy (Eq. (??)) yields :

$$B(z) \approx \frac{g}{T_e(z)} \frac{g}{T_e} \int_0^z \frac{dp}{p_s} \delta \Gamma_e(z) dz - \Gamma_m(z) dz \quad (26)$$

322 The lapse rate of the entraining environment, where $\delta \Gamma = \Gamma_e - \Gamma_m$. We use the entraining lapse rate
 323 Γ_e , can be derived from the conservation of entraining moist static energy following Eq. (B18) in
 324 ?. This yields: as in ?, but expressed in pressure coordinates:

$$\Gamma_e = \frac{g}{c_p} + \frac{L_v}{c_p(1+a)} \frac{dq_s}{dz} \Gamma_d \cdot \frac{(1+a)\alpha_d + \alpha_L}{(1+a)c_{pd} + c_L} \quad (27)$$

325 where a is a dimensionless entrainment parameter. Here, we use $a = 0.2$ following ?. The difference
 326 between the environmental and parcel lapse rates is therefore directly proportional to the vertical

327 moisture gradient:

$$\Gamma_e(z') - \Gamma_m(z') = \left(\frac{1}{1+a} - 1 \right) \frac{L_v}{c_p} \frac{dq_s}{dz} = -\frac{a}{1+a} \frac{L_v}{c_p} \frac{dq_s}{dz}$$

328 Substituting Eq. (??) and Eq. (???) into Eq. (??) shows that and simplifying gives

$$B = \underbrace{\frac{g}{T_e} \int_{p_s}^p \Gamma_d \cdot \frac{a(1-k)\tilde{c}}{(1+a+\tilde{c})(1+\tilde{c})} dp'}_{(28)}$$

329 Under the simplifying assumption that entrainment parameter a is constant with T_s , T_e increases
 330 monotonically with T_s at all p . Then the origin of the same physical mechanism used to explain the
 331 non-monotonicity in moist adiabatic warming applies for buoyancy: of B must be in the integrand,
 332 $\delta\Gamma$. B depends on T primarily through \tilde{c} , which scales exponentially with T through q^* , whereas
 333 Γ_d and k are linear functions of T . In the limit of $\tilde{c} \rightarrow 0$ (cold and dry), $\delta\Gamma$ scales as \tilde{c} , which
 334 increases with T . In the limit of $\tilde{c} \rightarrow \infty$ (warm and humid), $\delta\Gamma$ scales as \tilde{c}^{-1} , which decreases with
 335 increasing T . This means $\delta\Gamma$ maximizes at some intermediate \tilde{c} .

336 To solve for the condition that maximizes buoyancy we solve for the \tilde{c} derivative of the integrand
 337 $\delta\Gamma$ in Eq. (??) and set it to zero:

$$B(z) = -\frac{g}{T_e(z)} \frac{d}{d\tilde{c}} \left(\frac{a}{1+a} \frac{L_v}{c_p} \Gamma_d \cdot \frac{a(1-k)\tilde{c}}{(1+a+\tilde{c})(1+\tilde{c})} \right) \int_0^z \frac{dq_s}{dz'} dz' = 0 \quad (29)$$

338 This shows that If we assume that a , k , and Γ_d do not vary with T , the solution to Eq. (??) is

$$\tilde{c}_{\text{peak}} = \sqrt{1+a} \quad (30)$$

339 Thus the condition that maximizes buoyancy is $c_L = \sqrt{1+a} c_{pd}$. In the limit of weak entrainment
 340 $a \rightarrow 0$, this reduces to $c_L = c_{pd}$. In the presence of entrainment, buoyancy is directly proportional to
 341 the vertical integral of the moisture gradient, dq_s/dz . Since dq_s/dz is composed of the competing
 342 Cooling and Pressure terms, it follows that buoyancy is governed by the same mechanism. peaks
 343 at a higher c_L and so higher T_s all else equal. Entrainment dilutes the air parcel and reduces the
 344 latent heat released by the cooling parcel given the same q^* . The factor $\sqrt{1+a}$ describes the shift

345 in the critical point separating the vapor limited and cooling limited regimes toward higher q^* in
 346 the presence of entrainment.

347 Numerical calculations confirm this expectation. The results show that buoyancy at a fixed height
 348 first increases and then decreases as the How important is the factor $\sqrt{1+a}$? For an entrainment
 349 rate representative of Earth's current climate $a = 0.2$, the difference in T_s increases (of $c_L = c_{pd}$
 350 and $c_L = \sqrt{1+a}c_{pd}$ are < 1.49 K (compare red and solid black lines in Fig. ??a). This difference
 351 decreases with height and becomes insignificant around the tropopause (0.46 K at $p = 200$ hPa).
 352 This is why the criterion $c_L = c_{pd}$ works well for explaining the non-monotonicity of CAPE for
 353 present Earth-like climates (?). However, for stronger entrainment rates and for understanding the
 354 non-monotonicity of buoyancy in the lower troposphere, the factor $\sqrt{1+a}$ becomes more important
 355 (e.g., 4.38 K for $a = 0.7$ at the surface; compare red and solid black lines in Fig. ??). Decomposing
 356 the total buoyancy into the two components reveals the source of this behavior (??b).

357 How well do these criteria capture the T_s that maximizes buoyancy across the troposphere? We
 358 first focus on $\delta\Gamma$, i.e. the integrand in Eq. (??). For $a = 0.2$, both criteria capture the T_s of peak
 359 $\delta\Gamma$ well (< 1.39 K for $c_L = \sqrt{1+a}c_{pd}$, < 2.87 K for $c_L = c_{pd}$, compare red and solid black lines
 360 to dashed line in Fig. ??a). The total buoyancy, B_{total} , is the sum of the contributions from the
 361 Cooling Term (B_{cool}) and the Pressure Term (B_{pres}):

$$B_{\text{cool}}(z) = -\frac{g}{T_e(z)} \left(\frac{a}{1+a} \frac{L_v}{c_p} \right) \int_0^z \left(-\Gamma_m \frac{\partial q_s}{\partial T} \right) dz'$$

$$B_{\text{pres}}(z) = -\frac{g}{T_e(z)} \left(\frac{a}{1+a} \frac{L_v}{c_p} \right) \int_0^z \left(-\rho g \frac{\partial q_s}{\partial p} \right) dz'$$

$$B_{\text{total}}(z) = B_{\text{cool}}(z) + B_{\text{pres}}(z)$$

362 The Cooling Term provides a positive buoyancy contribution that increases monotonically with
 363 surface temperature, while the Pressure Term provides a negative buoyancy contribution that also
 364 grows in magnitude. The sum of these two opposing effects produces the small error arises even for
 365 the $c_L = \sqrt{1+a}c_{pd}$ criterion because $\Gamma_d(1-k)$ is weakly non-monotonic behavior of buoyancy.
 366 with T (Γ_d increases with T and $(1-k)$ decreases with T), which we ignored earlier in order to
 367 analytically solve Eq. (??). This error is amplified as we integrate $\delta\Gamma$ to obtain buoyancy Eq. (??)

368 because the error in T_s of peak $\delta\Gamma$ from levels below p accumulates for the T_s of peak B (compare
 369 red and solid black lines to dotted line in Fig. ??a).

370 ~~This non-monotonic behavior of buoyancy~~ For a higher entrainment parameter $a = 0.7$ the
 371 importance of the factor $\sqrt{1+a}$ becomes clear. The error in T_s of peak $\delta\Gamma$ is < 3.39 K for the
 372 $c_L = \sqrt{1+ac_{pd}}$ criterion compared to < 5.83 K for the $c_L = c_{pd}$ criterion (compare red and solid
 373 black lines to dashed line in Fig. ??b). The error in T_s of peak buoyancy is lower for the $c_L = c_{pd}$
 374 criterion (< 3.37 K) compared to the $c_L = \sqrt{1+ac_{pd}}$ criterion (< 4.66 K, compare red and solid
 375 black lines to dotted black line in Fig. ??b). This is because $c_L = c_{pd}$ underpredicts T_s for peak B in
 376 the lower troposphere, which offsets the growth of the larger error in peak $\delta\Gamma$ (compare solid black
 377 and dotted lines in Fig. ??b). The criterion $c_L = c_{pd}$ predicts the T_s of peak buoyancy better than
 378 $c_L = c_{pd}\sqrt{1+a}$ in some cases because of a cancelation of errors rather than for the right physical
 379 reason. For example the criterion $c_L = c_{pd}$ predicts no shift in T_s that maximizes B to variations
 380 in a while the criterion $c_L = \sqrt{1+ac_{pd}}$ qualitatively captures the shift in peak $\delta\Gamma$ and B toward
 381 warmer T_s with increasing entrainment (Fig. ??c).

382 ~~The non-monotonicity of buoyancy with surface temperature~~ extends to the strength of the
 383 convective updraft. We model the updraft's specific kinetic energy, $\frac{1}{2}w^2$, using Eq. (1) from ?:

$$\frac{d}{dz} \left(\frac{1}{2}w^2 \right) = a'B(z) - (1+b')\epsilon(z)w^2 \quad (31)$$

390 where a' and b' are dimensionless constants. We use $a' = 1/6$ and $b' = 2/3$ following ?. $\epsilon(z)$ is
 391 ~~We calculate~~ the fractional entrainment rate, ~~which is calculated~~ $\epsilon(z)$ following Eq. (3) in ? with
 392 entrainment parameter $a = 0.2$ and precipitation efficiency $PE = 0.35$. Since $w(z)$ is determined
 393 by the integral of the net force, which includes buoyancy, we expect ~~the non-monotonic dependence~~
 394 ~~on T_s extends to the vertical velocity profile as well~~ updraft velocity to also vary non-monotonically
 395 ~~with surface temperature~~.

396 Numerically integrating Eq. (??) confirms this expectation. Updraft velocity varies
 397 non-monotonically with T_s , updraft velocity decreases with surface temperature at lower levels
 398 while it increases with surface temperature at higher levels (Fig. ??a). The ~~resulting vertical velocity~~
 399 ~~profiles exhibit a clear non-monotonic dependence on T_s . Because~~ surface temperature of peak

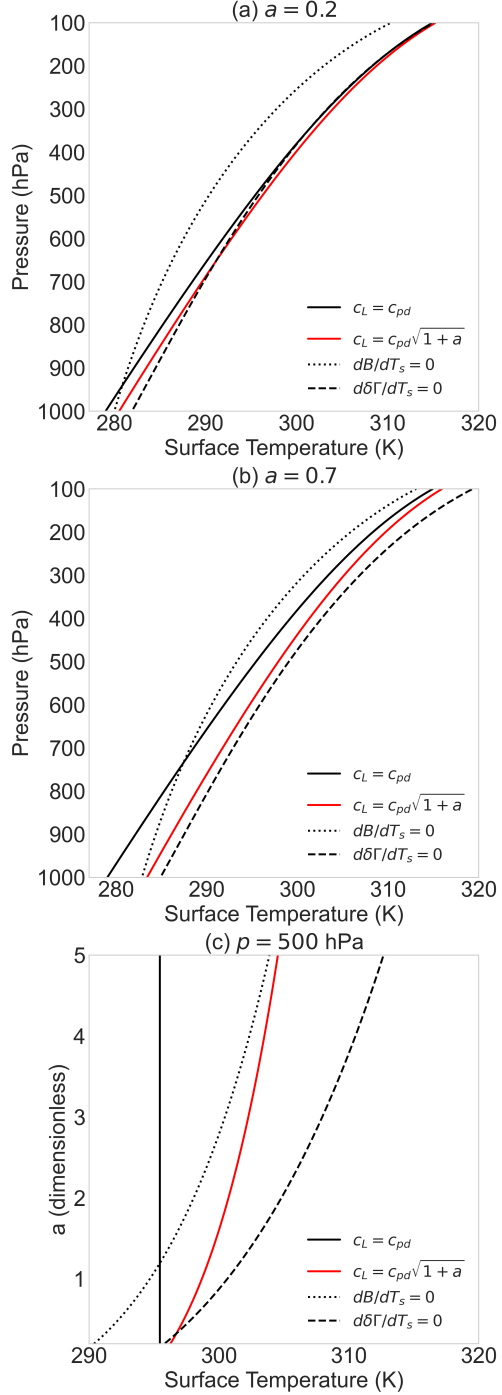


FIG. 6. Surface temperature T_s corresponding to the criterion $c_L = c_{pd}$ (solid black), the criterion $c_L = c_{pd}\sqrt{1+a}$ (red), the maximum of buoyancy B (dotted), and the minimum of the difference between an entraining lapse rate and moist-adiabatic lapse rate $\delta\Gamma = \Gamma_e - \Gamma_m$ (dashed) for the entrainment parameter (a) $a = 0.2$ and (b) $a = 0.7$. (c) The criterion $c_L = c_{pd}\sqrt{1+a}$ captures the a dependence of $\delta\Gamma$ and B extrema evaluated at pressure $p = 500$ hPa. In comparison the criterion $c_L = c_{pd}$ is not sensitive to the entrainment parameter a (vertical black line).

400 updraft velocity increases at higher levels, consistent with the non-monotonicity of moist-adiabatic
 401 warming and buoyancy (Fig. ??b).

402 Is this result relevant to Earth's atmosphere, where convective thermodynamics is not strictly
 403 moist-adiabatic and dynamics is subject to details and constraints not considered here such as cloud
 404 microphysics, radiative transfer, and turbulence? There are examples in the literature that show both
 405 buoyancy and updraft velocity diagnosed from cloud-resolving models vary non-monotonically
 406 with surface temperature. Buoyancy profiles simulated by Das Atmosphärische Modell and
 407 predicted by the zero-buoyancy plume model agree well across a large range of surface temperature
 408 (Fig. 2a in ?). Updraft velocity profiles simulated by CM1 (Fig. 2 in ?) is qualitatively consistent
 409 with Eq. (??) is non-linear, the contributions from the two buoyancy terms are not simply additive.
 410 We therefore isolate the influence of each term by first calculating the velocity driven by the Cooling
 411 Term's positive buoyancy alone (w_{cool}), and then calculating the effect of but there are quantitative
 412 differences. CM1 simulates a decrease in updraft velocity with T_s below 900 hPa while Eq. (??)
 413 predicts a decrease in vertical velocity with T_s below a much deeper layer, $z \approx 11$ km at 300 K. To
 414 understand the applicability and robustness of the Pressure Term (w_{pres}) as the residual required to
 415 recover the total velocity (w_{total}):

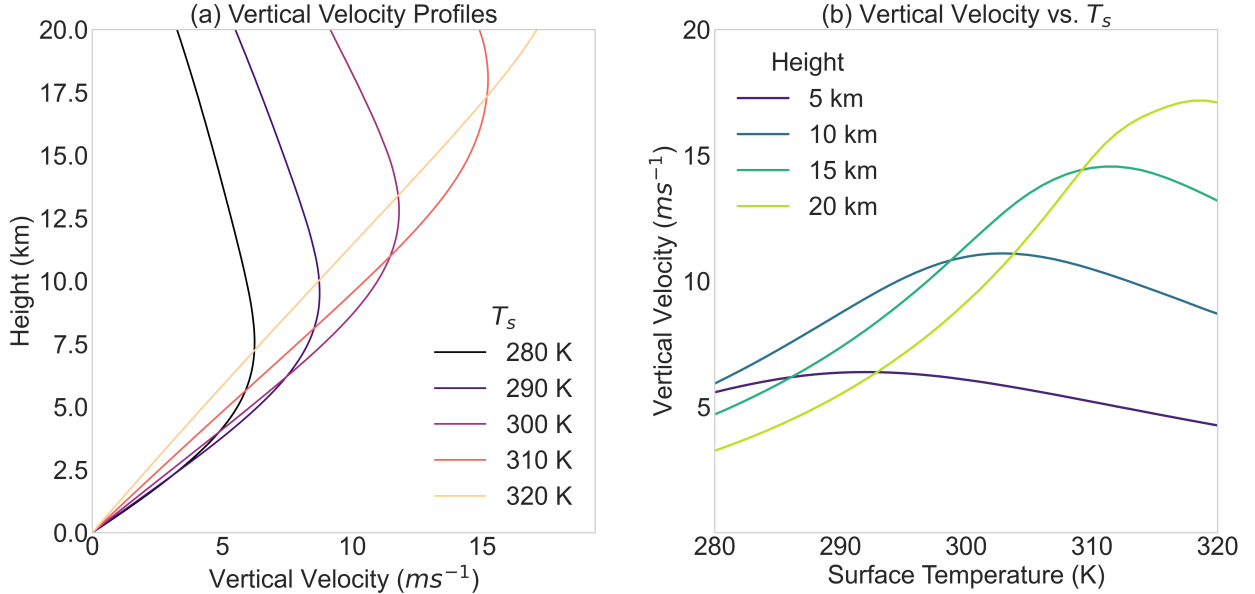
$$\frac{d}{dz} \left(\frac{1}{2} w_{\text{cool}}^2 \right) = a' B_{\text{cool}}(z) - (1 + b') \epsilon(z) w_{\text{cool}}^2$$

$$w_{\text{pres}}(z) = w_{\text{total}}(z) - w_{\text{cool}}(z)$$

416 This decomposition (Fig. ??) shows that the monotonically increasing velocity from the Cooling
 417 Term is counteracted by an increasingly strong opposing effect from the Pressure Term, resulting in
 418 non-monotonicity in updraft velocity predicted by Eq. (??). we analyzed 9 cloud-resolving models
 419 simulating radiative convective equilibrium in a 100 km x 100 km domain from the RCEMIP
 420 project (?). We define updraft velocity as the mean of vertical velocity w exceeding the 99.9th
 421 percentile ($w > 99.9$) at each height for w aggregated over horizontal space and the last 25 days of
 422 each simulation. The 99.9th percentile corresponds to the non-monotonic total response. fastest
 423 1000 samples of w per level per model run. We focus on the strongest convective updrafts because
 424 a moist-adiabatic profile is most relevant for the convective core of the strongest updrafts (?).

(a) Vertical profiles of buoyancy for an undiluted parcel ascending through an environment set by an entraining plume, calculated for several surface temperatures. (b) Buoyancy at fixed heights as a function of surface temperature. The entraining environmental profile follows ?.

The total buoyancy from Fig. ?? is decomposed into contributions from the Cooling and Pressure terms. (a,b) The contribution to buoyancy from the Cooling Term, which provides a positive, monotonically increasing forcing. (c,d) The contribution from the Pressure Term, which provides a negative (suppressing) forcing that grows in magnitude with temperature.



(a) Vertical profiles of updraft velocity, calculated by numerically integrating Eq. (??) using the total buoyancy from Fig. ???. (b) Updraft velocity at fixed heights as a function of surface temperature. The velocity exhibits a clear non-monotonic dependence on surface temperature, consistent with the behavior of buoyancy.

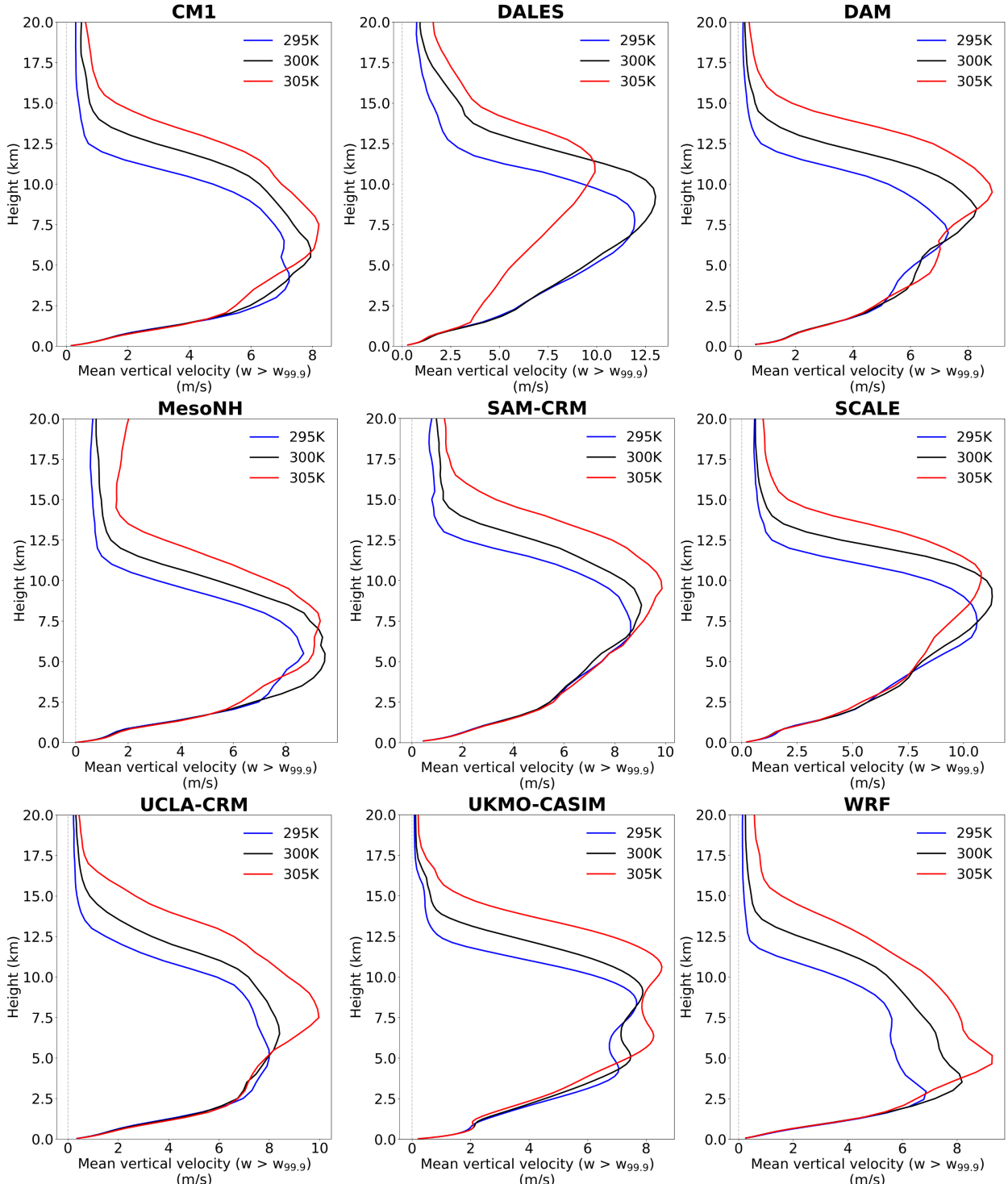
425 FIG. 7. (a) Vertical profiles of updraft velocity, calculated by numerically integrating Eq. (??) in height using
 426 buoyancy B from Eq. (??). Updraft velocity decreases with surface temperature at lower levels while it increases
 427 with surface temperature at higher levels. (b) Updraft velocity varies non-monotonically with surface temperature
 428 at all levels, e.g. at 5, 10, 15, and 20 km. Updraft velocity peaks at warmer surface temperatures at higher levels
 429 consistent with the behavior of buoyancy (Fig. ??a) and moist-adiabatic warming (Fig. ??).

430 There is a large diversity of updraft velocity in the RCEMIP simulations to variations in surface
 431 temperature (295, 300, and 305 K, see Fig. ??). Some models exhibit a clear shift toward
 432 increasingly top-heavy updraft velocity profiles with warming (e.g., CM1, DAM, UCLA-CRM,
 433 UKMO, WRF). In these models, updraft velocity decreases at lower levels, which is qualitatively
 434 consistent with Eq. (??) (Fig. ??a). SAM shows a top-heavy shift in updraft velocity without
 435 a clear decrease in lower levels. In the remaining models updraft velocity is non-monotonic
 436 with T_s but the T_s of peak updraft velocity does not increase to higher levels as expected from

Eq. (??) (Fig. ??b). For example DALES and SCALE predict a non-monotonic response in updraft velocity with T_s at $z \approx 8$ km but the peak updraft velocity weakens from $T_s = 300$ to 305 K. MesoNH also predicts a decrease in peak updraft velocity from $T_s = 300$ K to 305 K but predicts a non-monotonic response in updraft velocity with T_s at $z \approx 3$ km, much lower than in DALES and SCALE. The diversity of updraft velocity profiles likely emerges from differences in model details such as parameterization schemes for cloud microphysics, radiative transfer, and turbulence in addition to emergent behavior such as convective organization. Nonetheless, the presence of non-monotonicity in all but one model suggests that the simple mechanism controlling non-monotonicity in moist-adiabatic warming may be playing a role in shaping the variation of updraft velocity profiles across surface temperature in models that explicitly resolve convective storms.

4. Summary and Discussion

This paper presents a thermodynamic explanation for the non-monotonicity of moist adiabat warming. moist-adiabatic warming varies non-monotonically with respect to initial surface temperature. The non-monotonicity arises through the competing influences of a Cooling Term and a Pressure Term on the sensitivity of the moist adiabatic lapse rate. While both terms are proportional to the saturation specific humidity (q_s), which increases nearly exponentially with temperature, they are modulated by prefactors with different inverse temperature dependencies. The Cooling Term is proportional to q_s/T^2 , while the Pressure Term is proportional to q_s/T . The non-monotonic response arises because the stronger $1/T^2$ dependence of the Cooling Term's prefactor causes its influence to weaken relative to that of the Pressure Term as occurs because of a competition between two limiting factors of condensation: availability of water vapor and adiabatic cooling. At low temperature, condensation is limited by the availability of water vapor and moist-adiabatic warming scales like Clausius-Clapeyron. At high temperature, condensation is limited by the diminishing net cooling with ascent because high latent heating cancels an increasingly larger fraction of adiabatic cooling. In other words, the climate warms, leading to a crossover in their relative sensitivity to surface warming. The same mechanism for lapse rate sensitivity cascades to explain the non-monotonic behavior of convective buoyancy and vertical velocity as a function of T_s .



448 FIG. 8. The total vertical Updraft velocity is decomposed to show the influence of the Cooling from 9
 449 cloud-resolving models (CM1, DALES, DAM, MesoNH, SAM-CRM, SCALE, UCLA-CRM, UKMO-CASIM,
 450 and Pressure terms WRF) that participated in RCEMIP (?). The simulations are on a 100 km × 100 km periodic
 451 domain for uniform sea surface temperatures set to 295 (blue), 300 (black), and 305 K (red). Updraft
 452 velocity profile resulting from at each level is the positive buoyancy mean of vertical velocities w that exceed the
 453 Cooling Term alone. 99.9th percentile ($w_{99.9}$, defined separately for each model) The effect of the Pressure

Our findings on buoyancy complement the work of ?, who first explained the moist enthalpy response to warming is dominated by an increase in sensible enthalpy at low temperature and an increase in latent enthalpy at high temperature. The repartitioning of the dominant term in the moist enthalpy response to warming ($c_L = c_{pd}$) corresponds to where moist-adiabatic warming peaks. The non-monotonicity of CAPE. The two studies offer different but complementary insights. ? focused on explaining moist-adiabatic warming propagates to buoyancy as predicted by the zero-buoyancy plume model because the repartitioning of the moist enthalpy response from sensible to latent enthalpy with increasing temperature occurs in both entraining and moist-adiabatic lapse rates. The surface temperature where the buoyancy peaks follows $c_L = c_{pd}\sqrt{1+a}$, where a is the entrainment parameter as defined in ?. The non-monotonicity of buoyancy also propagates to updraft velocity. Cloud-resolving models simulating radiative-convective equilibrium exhibit diverse but qualitatively consistent responses of strong convective updrafts to surface temperature changes as predicted by the zero-buoyancy plume model.

The $c_L = c_{pd}$ criterion was first used to explain why buoyancy profiles are top heavy (?). Buoyancy maximizes where the saturation moist static energy difference between the environment and parcel (δh^*) is expressed as a temperature difference (sensible enthalpy difference, $c_{pd}\delta T$) rather than a humidity difference (latent enthalpy difference, $L_v\delta q^*$). The ratio $\tilde{c} = c_L/c_{pd} = L_v\delta q^*/(c_{pd}\delta T)$ quantifies the transition where δh^* is expressed largely in terms of $L_v\delta q^*$ (lower troposphere, where $\tilde{c} > 1$) and in terms of $c_{pd}\delta T$ (upper troposphere, where $\tilde{c} < 1$). and ? explained the non-monotonicity of buoyancy at the tropopause as a proxy for CAPE. Here, we focus on explaining the to explain the non-monotonicity of CAPE with surface temperature. Following the same reasoning as in ?, ? shows that tropopause buoyancy and CAPE peak where $c_L = c_{pd}$. We show that a more general criterion for the T_s of peak buoyancy is $c_L = c_{pd}\sqrt{1+a}$, which reduces to $c_L = c_{pd}$ in the limit of weak entrainment. The factor $\sqrt{1+a}$ is insignificant in Earth's current climate (e.g. for $a = 0.2$, $\sqrt{1+a} = 1.09$) so ?'s criterion works well for understanding the non-monotonicity of CAPE on present Earth-like atmospheres. However, the factor $\sqrt{1+a}$ is important for understanding the non-monotonicity of buoyancy at any fixed height. We also provide a different perspective on the source of non-monotonicity that arises from the competition in the sensitivity of a Cooling Term that favors condensation and a Pressure Term,

502 driven by decreasing ambient pressure, that opposes it lower levels and CAPE in a world with
503 stronger entrainment rates than on present Earth.

504 Curiously, the surface temperature of peak CAPE (≈ 335 K, ?) is similar to the surface
505 temperature that marks the transition to a moist greenhouse regime (≈ 335 K, ???). Is this
506 similarity due to a shared physical mechanism or a coincidence? The criterion for peak CAPE
507 is $L_v(\partial_T q^*)|_{t=c_{pd}}$, i.e. the surface temperature where the *temperature sensitivity* of latent and
508 sensible enthalpy at the *tropopause* are equal. On the other hand the criterion for the transition to a
509 moist greenhouse is $L_v q_s^* = c_{pd} T_s$, i.e. the surface temperature where the *magnitude* of latent and
510 sensible enthalpy at the *surface* are equal (?). The ratio of the temperature sensitivity of latent and
511 sensible enthalpy at the tropopause scales differently from the ratio of the magnitude of latent and
512 sensible enthalpy at the surface (Fig. ??, see Appendix D for more detail). While these thresholds
513 coincide around 335 K in Earth-like climates, their underlying scalings differ, suggesting that they
514 may diverge in other planetary climates.

515 The non-monotonicity of ~~moist adiabatic~~ moist-adiabatic warming may have additional impli-
516 cations for climate, such as the organization of convection and the large-scale circulation response
517 to warming. For example, ? explain the mechanism behind the $2\% \text{ K}^{-1}$ scaling of the mean
518 and extreme upper-level wind response to warming by assuming a moist-adiabatic atmosphere.
519 The non-monotonicity of ~~moist adiabatic~~ moist-adiabatic warming would drive a non-monotonic
520 change in the meridional and zonal temperature gradients at fixed height and pressure levels. This
521 could serve as a thermodynamically driven hypothesis for ~~understanding state dependence in the~~
522 ~~potential of non-monotonocities to emerge in dynamical responses to warming such as in~~ the re-
523 sponse of ~~Hadley and Walker Cells to warming~~ jet stream wind, extratropical cyclones, and mean
524 overturning circulations.

525 *Acknowledgments.* I thank the Union College Faculty Research Fund and the NSF National
526 Center for Atmospheric Research Advanced Studies Program for supporting this work. I thank
527 Andrew Williams, Jiawei Bao, Jonah Bloch-Johnson, Martin Singh, and Stephen Po-Chedley, Nadir
528 Jeevanjee, and two anonymous reviewers for helpful discussions and feedback on the manuscript.

529 *Data availability statement.* All scripts used for analysis and plots in this paper are available at
530 <https://github.com/omiyawaki/miyawaki-2025-nonmonotonic-moist-adiabat>. They
531 will also be archived on Zenodo upon publication.

533 The moist adiabatic profiles are calculated

534 Calculating moist-adiabatic Profiles

535 We calculate moist-adiabatic profiles numerically by assuming that the conservation of saturation
 536 moist static energy (MSE) is conserved, where: \underline{h}^* :

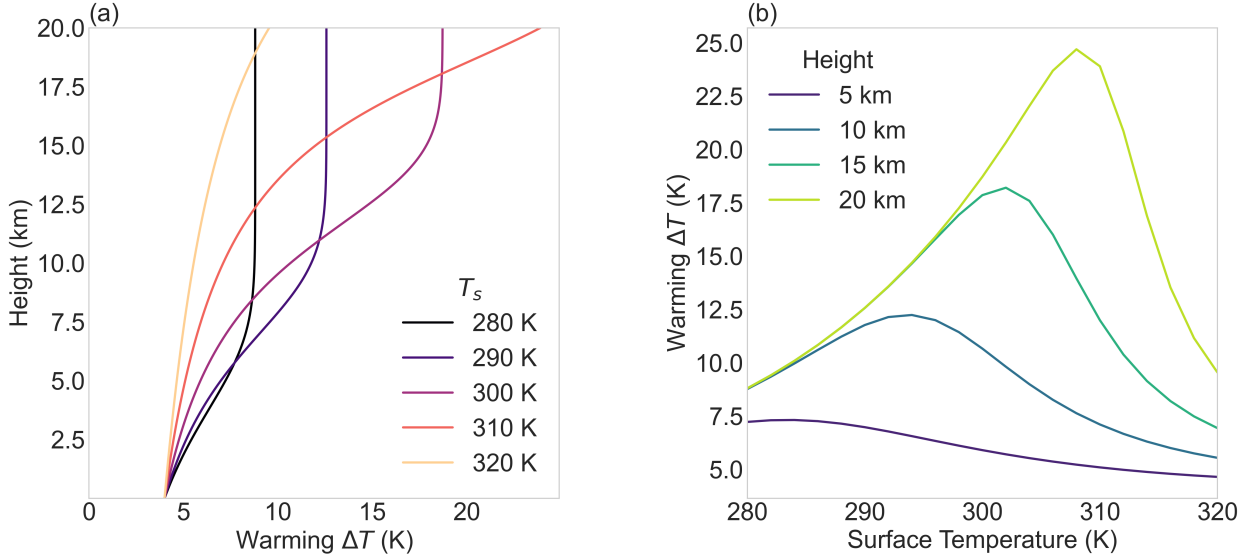
$$\text{MSE} \underline{h}^* = c_{pd} T + gz + L_v q_s^* \quad (\text{A1})$$

537 Here, where T is temperature, z is height, p is pressure, q_s is q^* is the saturation specific humidity,
 538 g is the acceleration due to gravity, c_{pd} is the specific heat of dry air at constant
 539 pressure, and L_v is the latent heat of vaporization. All thermodynamic constants are defined in
 540 Table ???. Saturation vapor pressure is calculated using We use the ? formula for saturation vapor
 541 pressure e^* (Eq. (10) in ?).

542 The calculation proceeds in discrete vertical steps of Δz (100 m). For ???. The values we use
 543 for all thermodynamic constants are in Table ???.

544 We first calculate surface saturation moist static energy \underline{h}_s^* for a given surface temperature (T_s)
 545 and surface pressure (p_s). MSE is calculated at the surface ($z = 0$) and is held constant over height
 546 . At each subsequent height step. We calculate \underline{h}^* at higher levels in -50 hPa pressure increments.
 547 We assume hydrostatic balance to calculate the height z_{i+1} , the pressure at the next pressure
 548 level p_{i+1} is first calculated using hydrostatic balance. Then, a numerical root-finding algorithm
 549 (scipy.optimize.root_scalar with the Brentq method) is used to find the temperature. We solve for
 550 T_{i+1} that satisfies the condition that the MSE at $(T_{i+1}, p_{i+1}, z_{i+1})$ is equal to the surface MSE $\underline{h}_{i+1}^* = \underline{h}_s^*$
 551 using Brent's root-finding method (scipy.optimize.root_scalar with method=brentq).

552 To We also show moist-adiabatic warming in height coordinates to demonstrate that the
 553 non-monotonic warming is independent of the vertical coordinate, the results are also presented
 554 in pressure coordinates non-monotonicity is not an artifact of the choice of the vertical coordinate
 555 (Fig. ??). These profiles are obtained by interpolating the temperature profiles for the base and
 556 perturbed climates onto a common pressure grid. The warming profile in pressure coordinates,
 557 $\Delta T(p)$, is the difference between these two interpolated temperature profiles We follow the same
 558 procedure as above except we step to higher levels in 100 m height increments.



559 FIG. A1. The moist adiabatic warming response to a 4 K surface warming in pressure coordinates. (a)
560 Vertical profiles of the temperature response (ΔT) as moist-adiabatic warming to a function of pressure for 4 K
561 surface temperatures (T_s) of warming for $T_s = 280, 290, 300, 310$, and 320 K. Warming decreases with initial
562 surface temperature at lower levels while it increases with initial surface temperature at higher levels. (b) The
563 moist-adiabatic warming (ΔT) varies non-monotonically with initial surface temperature at fixed pressure all
564 levels of 500, 400 e.g. at 5 km, 300 10 km, 15 km, and 200 hPa as a function of T_s . The non-monotonic behavior
565 seen in height coordinates (Fig. 20 ??e) is also evident in pressure coordinates km. moist-adiabatic warming
566 peaks at warmer initial surface temperatures at higher levels.

TABLE A1. Thermodynamic constants used in the calculation of moist adiabatic profiles this study.

Symbol	Description	Value	Units
g	Acceleration due to gravity	9.81	m s^{-2}
c_p, c_{pd}	Specific heat of dry air	1005.7	$\text{J kg}^{-1} \text{K}^{-1}$
R_d	Gas constant for of dry air	287.05	$\text{J kg}^{-1} \text{K}^{-1}$
R_v	Gas constant for of water vapor	461.5	$\text{J kg}^{-1} \text{K}^{-1}$
ϵ	Ratio of gas constants (R_d/R_v)	0.622	dimensionless
p_s	Reference surface pressure	100,000–1000	Pa–hPa
L_v	Latent heat of vaporization	2.501×10^6	J kg^{-1}

567

APPENDIX B

568

Sensitivity of Non-monotonicity to Fusion

569 We assess how latent heat of fusion influences the non-monotonicity of moist-adiabatic warming.
 570 Following ?, we represent freezing following the IFS Cycle 40 documentation (?). The fraction of
 571 liquid water α varies with T as follows

$$\alpha(T) = \begin{cases} 0, & T \leq T_{\text{ice}} \\ \left(\frac{T - T_{\text{ice}}}{T_0 - T_{\text{ice}}} \right)^2 & T_{\text{ice}} < T < T_0 \\ 1 & T \geq T_0 \end{cases} \quad (\text{B1})$$

572 where $T_{\text{ice}} = 253.15 \text{ K}$ and $T_0 = 273.15 \text{ K}$. All condensate is ice below 253.15 K , all condensate is
 573 liquid above 273.15 K , and the transition between the two limits is quadratic.

574 The saturation vapor pressure e^* is the weighted average over liquid (e_{ℓ}^*) and ice (e_i^*):

$$e^* = \alpha e_{\ell}^* + (1 - \alpha) e_i^* \quad (\text{B2})$$

575 The saturation vapor pressure over liquid and ice is

$$e_{\ell,i}^*(T) = a_1 \exp \left(a_3 \frac{T - T_0}{T - a_4} \right) \quad (\text{B3})$$

576 where over liquid $a_1 = 611.21 \text{ Pa}$, $a_3 = 17.502$, $a_4 = 32.19 \text{ K}$ (?) and over ice $a_1 = 611.21 \text{ Pa}$,
 577 $a_3 = 22.587$, $a_4 = -0.7 \text{ K}$ (?).

578 The effective latent heat of vaporization $L_e^*(T)$ includes both condensation and fusion:

$$L_e^*(T) = L_v + (1 - \alpha) L_f \quad (\text{B4})$$

579 where $L_f = 0.334 \times 10^6 \text{ J kg}^{-1}$ is the latent heat of fusion.

580 Moist adiabats including fusion are obtained by solving for T that conserves the saturation moist
 581 static energy with the effective latent heat L_e :

$$h_{\text{fusion}}^* = c_{pd} T + gz + L_e q^* \quad (\text{B5})$$

582 The non-monotonicity of moist-adiabatic warming emerges with or without fusion (compare
 583 Fig. ??b and ??a). Fusion introduces a secondary local maximum of warming due to the additional
 584 local energy release from fusion (Fig. ??b). When the secondary peak is to the right of the primary
 585 peak the T_s of peak warming shifts to colder T_s (points below the 1:1 line in Fig. ??c). As the
 586 secondary peak overlaps with the primary peak, the T_s of peak warming shifts to warmer T_s with
 587 fusion (points above the 1:1 line in Fig. ??c). This effect is largest (6.01 K) at 727 hPa. Since fusion
 588 represents a secondary effect and complicates the analysis, we neglect it in the main analysis.

594 APPENDIX C

595 Sensitivity of Non-monotonicity to Saturation Vapor Pressure Formulas

596 The moist-adiabatic lapse rate depends on the choice of the empirical formula for saturation vapor
 597 pressure e^* . To assess the sensitivity of the non-monotonicity in moist-adiabatic warming to
 598 different empirical fits of $e^*(T)$, we test how the T_s of peak warming varies across three formulas:
 599 ?, Goff-Gratch (as described in ?), and ?.

600 The ? formula is:

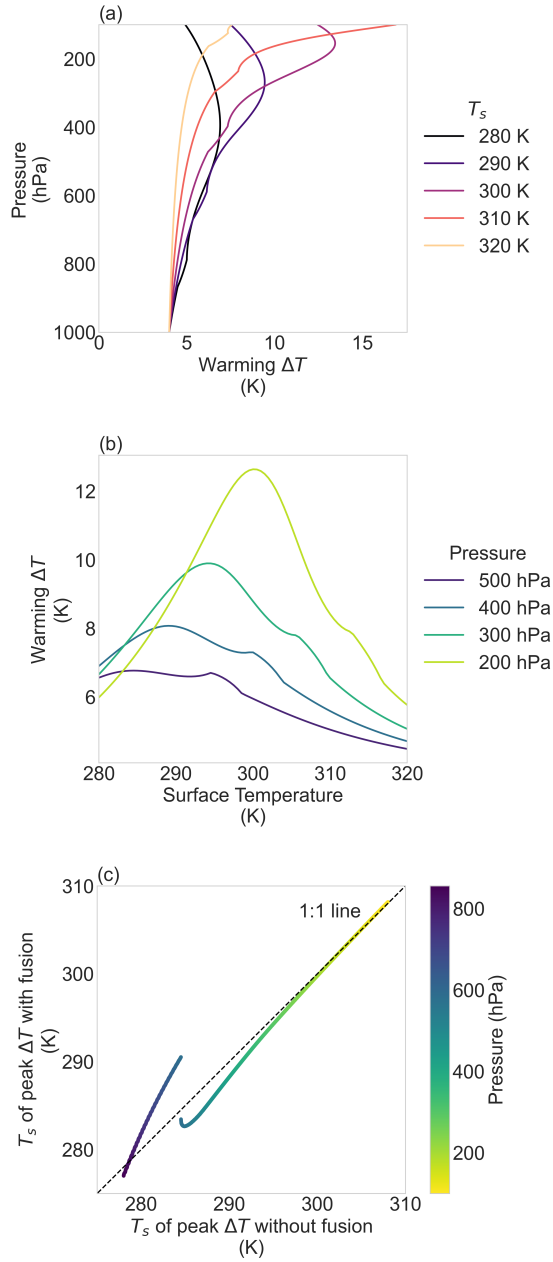
$$e^* = 6.112 \exp\left(\frac{17.67(T - 273.15)}{T - 29.65}\right) \quad [\text{hPa}] \quad (\text{C1})$$

601 The Goff-Gratch formula is:

$$\begin{aligned} \log_{10} e^* &= -7.90298 \left(\frac{373.16}{T} - 1 \right) + 5.02808 \log_{10} \left(\frac{373.16}{T} \right) \\ &\quad - 1.3816 \times 10^{-7} \left(10^{11.344(1-T/373.16)} - 1 \right) + 8.1328 \times 10^{-3} \left(10^{-3.49149(373.16/T-1)} - 1 \right) \\ &\quad + \log_{10}(1013.246) \quad [\text{hPa}] \quad (\text{C2}) \end{aligned}$$

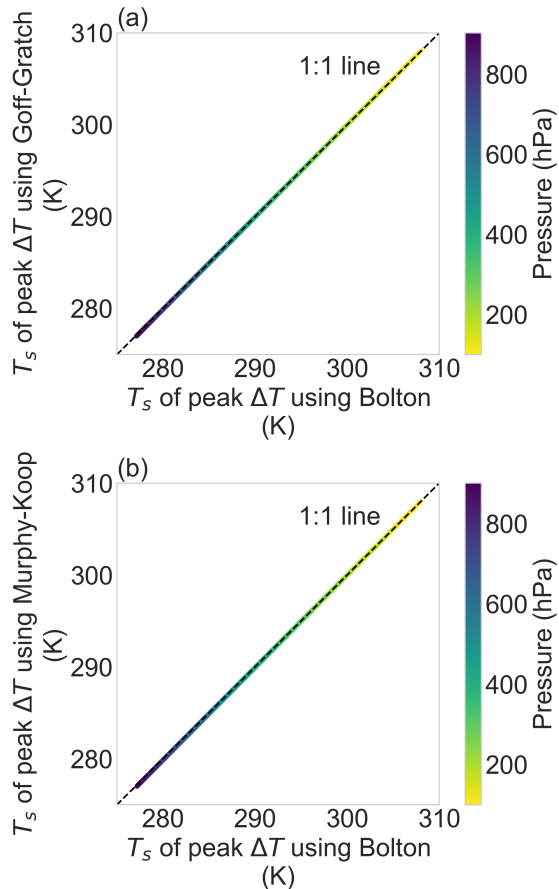
602 The ? formula is:

$$\begin{aligned} \ln e^* &= 54.842763 - \frac{6763.22}{T} - 4.210 \ln T + 0.000367T \\ &\quad + \tanh(0.0415(T - 218.8)) \left(53.878 - \frac{1331.22}{T} - 9.44523 \ln T + 0.014025T \right) \quad [\text{Pa}] \quad (\text{C3}) \end{aligned}$$



589 FIG. B1. moist-adiabatic warming ΔT for 4 K surface warming including latent heat of fusion. (a) Warming
590 decreases at lower levels with initial surface temperatures (T_s) while it increases at upper levels with T_s for 280,
591 290, 300, 310, and 320 K. (b) Warming peaks at warmer T_s at higher levels, e.g. at 500, 400, 300, and 200 hPa.
592 (c) T_s corresponding to peak warming with and without fusion are comparable at upper levels (> 500 hPa) but
593 can deviate up to 6.01 K at lower levels (< 500 hPa).

603 where T is in Kelvin for all 3 formulas.
 604 $?$ is sufficiently accurate for the purposes of evaluating the T_s that leads to maxima in
 605 moist-adiabatic warming (Fig. ??). The differences in peak T_s across the three saturation vapor
 606 pressure formulas are small. The largest difference in T_s of peak warming is 0.11 K at 903 hPa
 607 between Bolton and Goff-Gratch and 0.16 K at 901 hPa between Bolton and Murphy-Koop. We
 608 choose to use $?$ in the main analysis due to its simplicity.



609 FIG. C1. (a) T_s corresponding to peak warming using $?$ and Goff-Gratch saturation vapor pressure formula are
 610 similar (difference is < 0.11 K). (b) Same as (a) but comparing $?$ and $?$, which also predicts similar T_s of peak
 611 warming (difference is < 0.16 K).

612

APPENDIX D

613

Criteria for Moist Greenhouse and Peak CAPE

614 The moist greenhouse transition occurs when high water vapor concentration in the stratosphere
 615 leads to increased photolysis of water vapor and hydrogen escape. The criterion for the onset of
 616 this regime is when the magnitude of the latent to sensible enthalpy at the surface are equal (?):

$$\frac{L_v q_s^*}{c_{pd} T_s} = 1 \quad (\text{D1})$$

617 In contrast, peak CAPE corresponds to the surface temperature where the temperature sensitivity
 618 ratio of latent and sensible enthalpy at the tropopause are equal (which works well for $a \ll 1$, ?):

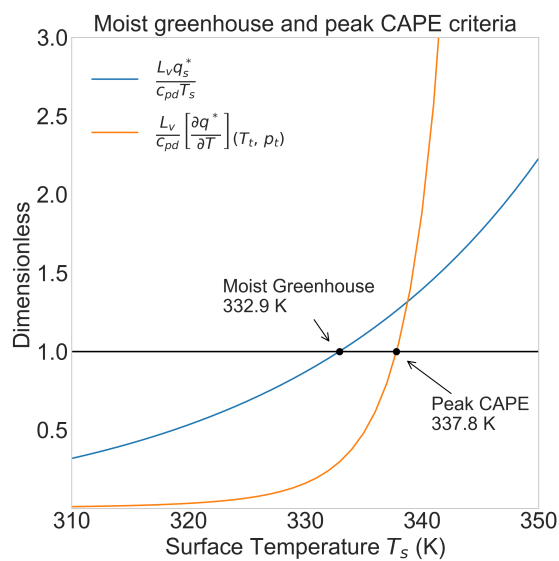
$$\frac{c_{L,t}}{c_{pd}} = \left. \frac{L_v}{c_{pd}} \frac{\partial q^*}{\partial T} \right|_t = 1 \quad (\text{D2})$$

619 where the subscript t is the tropopause. Combining Eq. (??) and Eq. (??) in this paper together
 620 with Eq. (15) in ?:

$$\left. \frac{dq^*}{dT} \right|_t \approx \frac{\epsilon}{p_s} \left(\frac{de_t^*}{dT} \exp(\mathcal{A}(T_s - T_t) + \mathcal{B}) - \mathcal{A} e^* \exp(\mathcal{A}(T_s - T_t) + \mathcal{B}) \right) \quad (\text{D3})$$

621 where $\mathcal{A} = \frac{c_{pd}}{R_d T_0}$, $\mathcal{B} = \frac{L_v q_s^*}{(1+a) R_d T_0}$, and $T_0 = \frac{T_s + T_t}{2}$. Following ? we set $a = 0$ and $T_t = 200$ K when
 622 calculating Eq. (??).

623 The T_s of the transition to the moist greenhouse regime (332.9 K, where the blue line equals
 624 1 in Fig. ??) and peak CAPE (337.8 K, where the orange line equals 1 in Fig. ??) are similar,
 625 both occurring ≈ 335 K. However, the T_s that satisfy each criteria emerge from nondimensional
 626 numbers that scale differently with T_s . The moist greenhouse criterion proposed by ? is only a
 627 function of surface moist enthalpy partitioning. The peak CAPE criterion is not only a function of
 628 surface moist enthalpy but also the tropopause temperature T_t , which is influenced by both moist
 629 thermodynamics and radiative transfer (e.g., ??). Thus there is no *a priori* expectation that the
 630 surface temperatures corresponding to these two transitions must coincide across a broad range of
 631 planetary climates.



632 FIG. D1. The T_s of the transition to a moist greenhouse regime and peak CAPE are both ≈ 335 K but they
 633 emerge from different criteria. The transition to a moist greenhouse regime corresponds to where the magnitude
 634 of latent and sensible enthalpy are equal (blue line equals 1). Peak CAPE corresponds to where the temperature
 635 sensitivity of latent and sensible enthalpy are equal (orange line equals 1).

636 **References**

- 637 Alduchov, O. A., and R. Eskridge, 1996: Improved magnus form approximation of saturation vapor
638 pressure. *Journal of Applied Meteorology*, **35** (4), 601–609.
- 639 Arakawa, A., and W. H. Schubert, 1974: Interaction of a cumulus cloud ensemble with the
640 large-scale environment, part I. *Journal of the Atmospheric Sciences*, **31** (3), 674–701.
- 641 Bao, J., V. Dixit, and S. C. Sherwood, 2022: Zonal temperature gradients in the tropical free
642 troposphere. *Journal of climate*.
- 643 Bolton, D., 1980: The computation of equivalent potential temperature. *Mon. Weather Rev.*,
644 **108** (7), 1046–1053.
- 645 Buck, A. L., 1981: New equations for computing vapor pressure and enhancement factor. *Journal*
646 *of Applied Meteorology and Climatology*, **20** (12), 1527–1532.
- 647 Byrne, M. P., and P. A. O’Gorman, 2013: Land–ocean warming contrast over a wide range of
648 climates: Convective quasi-equilibrium theory and idealized simulations. *Journal of climate*,
649 **26** (12), 4000–4016.
- 650 Del Genio, A. D., M.-S. Yao, and J. Jonas, 2007: Will moist convection be stronger in a warmer cli-
651 mate?: CONVECTION STRENGTH IN a WARMER CLIMATE. *Geophys. Res. Lett.*, **34** (16).
- 652 ECMWF, 2022: IFS documentation. Accessed: 2025-10-28, <https://www.ecmwf.int/en/publications/ifs-documentation>.
- 654 Emanuel, K. A., 1994: *Atmospheric Convection*. Oxford University Press.
- 655 Flannaghan, T. J., S. Fueglistaler, I. M. Held, S. Po-Chedley, B. Wyman, and M. Zhao, 2014:
656 Tropical temperature trends in atmospheric general circulation model simulations and the impact
657 of uncertainties in observed SSTs. *Journal of Geophysical Research, D: Atmospheres*, **119** (23),
658 13,327–13,337.
- 659 Hansen, J., A. Lacis, D. Rind, G. Russell, P. Stone, I. Fung, R. Ruedy, and J. Lerner, 1984: Cli-
660 mate sensitivity: Analysis of feedback mechanisms. *Climate Processes and Climate Sensitivity*,
661 American Geophysical Union (AGU), 130–163.

- 662 Held, I. M., 1982: On the height of the tropopause and the static stability of the troposphere.
663 *Journal of the Atmospheric Sciences*, **39** (2), 412–417.
- 664 Held, I. M., 1993: Large-scale dynamics and global warming. *Bull. Am. Meteorol. Soc.*, **74** (2),
665 228–242.
- 666 Held, I. M., and K. M. Shell, 2012: Using relative humidity as a state variable in climate feedback
667 analysis. *Journal of climate*, **25** (8), 2578–2582.
- 668 Held, I. M., and B. J. Soden, 2000: Water vapor feedback and global warming. *Annual review of*
669 *energy and the environment*, **25** (1), 441–475.
- 670 Hu, S., and G. K. Vallis, 2019: Meridional structure and future changes of tropopause height and
671 temperature. *Quarterly Journal of the Royal Meteorological Society*, **145** (723), 2698–2717.
- 672 Ingersoll, A. P., 1969: The runaway greenhouse: A history of water on venus. *Journal of the*
673 *atmospheric sciences*, **26** (6), 1191–1198.
- 674 Kasting, J., 1988: Runaway and moist greenhouse atmospheres and the evolution of earth and
675 venus. *Icarus*, **74**, 472–494.
- 676 Keil, P., H. Schmidt, B. Stevens, and J. Bao, 2021: Variations of tropical lapse rates in climate
677 models and their implications for upper tropospheric warming. *Journal of climate*, **34** (24), 1–50.
- 678 Komabayashi, M., 1967: Discrete equilibrium temperatures of a hypothetical planet with the
679 atmosphere and the hydrosphere of one component-two phase system under constant solar
680 radiation. *Journal of the Meteorological Society of Japan*, **45** (1), 137–139.
- 681 Levine, X. J., and W. R. Boos, 2016: A mechanism for the response of the zonally asymmetric
682 subtropical hydrologic cycle to global warming. *J. Clim.*, **29** (21), 7851–7867.
- 683 List, R. J., 1949: Smithsonian meteorological tables. *Smithsonian miscellaneous collections*, **114**,
684 1–521.
- 685 Manabe, S., and R. T. Wetherald, 1967: Thermal equilibrium of the atmosphere with a given
686 distribution of relative humidity. *J. Atmos. Sci.*, **24** (3), 241–259.

- 687 Miyawaki, O., Z. Tan, T. A. Shaw, and M. F. Jansen, 2020: Quantifying key mechanisms that
688 contribute to the deviation of the tropical warming profile from a moist adiabat. *Geophys. Res.*
689 *Lett.*, **47** (20), e2020GL089 136.
- 690 Murphy, D. M., and T. Koop, 2005: Review of the vapour pressures of ice and supercooled water
691 for atmospheric applications. *Quarterly journal of the Royal Meteorological Society. Royal*
692 *Meteorological Society (Great Britain)*, **131** (608), 1539–1565.
- 693 Neelin, J. D., and I. M. Held, 1987: Modeling tropical convergence based on the moist static energy
694 budget. *Mon. Weather Rev.*, **115** (1), 3–12.
- 695 O’Gorman, P. A., 2015: Precipitation extremes under climate change. *Current climate change*
696 *reports*, **1** (2), 49–59.
- 697 Riehl, H., and J. S. Malkus, 1958: On the heat balance of the equatorial trough zone. *Geophysica*,
698 **6** (3-4).
- 699 Romps, D. M., 2016: Clausius–Clapeyron scaling of CAPE from analytical solutions to RCE. *J.*
700 *Atmos. Sci.*, **73** (9), 3719–3737.
- 701 Santer, B. D., and Coauthors, 2005: Amplification of surface temperature trends and variability in
702 the tropical atmosphere. *Science*, **309** (5740), 1551–1556.
- 703 Seeley, J. T., and D. M. Romps, 2015: Why does tropical convective available potential energy
704 (CAPE) increase with warming? *Geophysical research letters*, **42** (23), 10,429–10,437.
- 705 Seeley, J. T., and D. M. Romps, 2016: Tropical cloud buoyancy is the same in a world with or
706 without ice. *Geophysical research letters*, **43** (7), 3572–3579.
- 707 Shaw, T. A., and O. Miyawaki, 2025: Moist adiabatic scaling explains mean and fast upper-level jet
708 stream wind response to climate change. *Geophysical research letters*, **52** (20), e2025GL118 315.
- 709 Shaw, T. A., and A. Voigt, 2016: What can moist thermodynamics tell us about circulation shifts
710 in response to uniform warming? *Geophysical research letters*, **43** (9), 4566–4575.
- 711 Singh, M. S., and P. A. O’Gorman, 2013: Influence of entrainment on the thermal stratification
712 in simulations of radiative-convective equilibrium. *Geophysical research letters*, **40** (16), 4398–
713 4403.

- 714 Singh, M. S., and P. A. O’Gorman, 2015: Increases in moist-convective updraught velocities with
715 warming in radiative-convective equilibrium. *Quarterly Journal of the Royal Meteorological*
716 *Society*, **141** (692), 2828–2838.
- 717 Vallis, G. K., P. Zurita-Gotor, C. Cairns, and J. Kidston, 2015: Response of the large-scale structure
718 of the atmosphere to global warming. *Quart. J. Roy. Meteor. Soc.*, **141** (690), 1479–1501.
- 719 Wing, A. A., K. A. Reed, M. Satoh, B. Stevens, S. Bony, and T. Ohno, 2018: Radiative–convective
720 equilibrium model intercomparison project. *Geoscientific Model Development*, **11** (2), 793–813.
- 721 Wordsworth, R. D., and R. T. Pierrehumbert, 2013: WATER LOSS FROM TERRESTRIAL
722 PLANETS WITH CO₂-RICH ATMOSPHERES. *The Astrophysical Journal*, **778** (2), 154.